Optimizing Demand Response in Deregulated Electricity Markets: A Customer-Centric Game Theory Approach

By

Arman Goudarzi

M.Sc. in Electrical Engineering, Mapua University, Manila, 2012

A Report Submitted in Partial Fulfillment

of the Requirements for the Degree of

MASTER OF ENGINEERING

in the Department of Electrical and Computer Engineering

Supervisory Committee

Optimizing Demand Response in Deregulated Electricity Markets: A Customer-Centric Game Theory Approach

by

Arman Goudarzi

M.Sc. in Electrical Engineering, Mapua University, Manila, 2012

Supervisory Committee

Dr. Issa Traore, Supervisor

(Department of Electrical and Computer Engineering)

Dr. Tao Lu, Departmental Member

(Department of Electrical and Computer Engineering)

Abstract

In the era of IoT-enabled smart grid technologies and the ever-increasing integration of renewable energy sources, the need for efficient and customer-oriented demand response programs is becoming crucial for the stability and flexibility of power systems. In this regard, this report presents an innovative customer-centric game theory-based demand response (CC-GTDR) for managing electricity consumption during periods of high demand in a deregulated electricity market. The proposed CC-GTDR method exceptionally combines both incentive and price-based demand response programs while emphasizing customer benefits and flexibility of choice. A fuzzy analytic hierarchy process based on non-linear programming (FAHP-NLP) is employed to determine the optimum weightings of the designed multi-criteria objective function of the study. To solve the proposed model, a hybrid optimization algorithm is implemented, which merges enthusiasm-assisted teaching and learning-based optimization (EaTLBO) with an enhanced variant of particle swarm optimization (EPSO). The study investigates various dynamic pricing mechanisms, such as time-of-use pricing, real-time pricing, and their combinations, in deregulated electricity markets. The proposed approach demonstrates significant improvements in overall load and peak load reductions, as well as utility profit gains. Additionally, the integration of renewable energy sources (RESs) within the CC-GTDR and profit-based dynamic cost environmental economic dispatch (DCEED) model results in substantial reductions in NOx emissions. The developed CC-GTDR model contributes to a more resilient and efficient electrical system by prioritizing customer engagement and empowerment, ultimately enhancing grid reliability and facilitating the integration of renewable resources.

Keywords: Customer-centric DRP, Dynamic pricing mechanisms (ToU and RTP), Deregulated electricity market, dynamically combined environmental economic dispatch (DCEED), Hybrid optimization algorithm (TLBO and PSO).

Table of Contents

Glossary

Acronyms

ABCO	Artificial bee colony optimization
CC-GTDR	Customer-centric game-theoretic demand response
DSMS	Demand-side management strategies
EaTLBO	Enthusiasm aided teaching and learning based optimization
EPSO	Enhanced particle swarm optimization
FAHP	Fuzzy analytic hierarchical process
GA-PSO	Hybrid genetic algorithm and particle swarm optimization
GHG	Greenhouse gasses
GWOA	Gray wolf optimization algorithm
HSO	Harmony search optimization
RES	Renewable energy resources
PBCEED	Profit based- combined economic and emission dispatch
PV	Photovoltaic array
PVC	Power violation constraint
NLP	Non-linear programming
SO	System operator
SRR	Spinning reserve requirement
WTG	Wind turbine generator

Variables

a_i, b_i, c_i, d_i and e_i	Cost coefficients of i^{th} generating unit
$a_i^{resv}, b_i^{resv}, c_i^{resv}, d_i^{resv}$ and e_i^{resv}	Reserve cost coefficients of i^{th} generating unit at time t
$\alpha_i^{SO_2}, \beta_i^{SO_2}, \gamma_i^{SO_2}, \eta_i^{SO_2}$ and $\delta_i^{SO_2}$	SO_2 coefficient emission volume of i^{th} generating unit
$\alpha_i^{NO_x}, \beta_i^{NO_x}, \gamma_i^{NO_x}, \eta_i^{NO_x}$ and $\delta_i^{NO_x}$	NO_x coefficient emission volume of i^{th} generating unit
$\alpha_i^{CO_2}, \beta_i^{CO_2}, \gamma_i^{CO_2}, \eta_i^{CO_2}$ and $\delta_i^{CO_2}$	CO_2 coefficient emission volume of i^{th} generating unit
α, β	Parameters of Beta distribution function
$C_i^{emi,t}$	Emission production cost of i^{th} generating unit at time t
$C_i^{Gen,t}$	Generation cost of i^{th} generating unit at time t
$C_i^{resv,t}$	Reserve cost of i^{th} generating unit at time t
$C_i^{WTG,t}$	Total generation cost of i^{th} WTG at time t
$C_i^{PV,t}$	Total generation cost of i^{th} PV at time t
$C_{Gen,i}^{WTG}$	Generation cost of i^{th} WTG
$C_{Gen,i}^{PV}$	Generation cost of i^{th} PV
$C_{Pen,i}^{AWP}$	Underestimation cost of available wind power of i^{th} WTG
$C_{Pen,i}^{APVP}$	Underestimation cost of available solar power of i^{th} PV
$C_{Pen,i}^{SR-WTG}$	Overestimation cost of SRR for i^{th} WTG
$C_{Pen,i}^{SR-PV}$	Overestimation cost of SRR for i^{th} PV
$d_{wind,i}$	Direct cost of i^{th} WTG
$d_{PV,i}$	Direct cost of i^{th} PV
$D(t)$	Load demand at time t
DR_i, UR_i	Downward and upward ramp-rate limit of i^{th}generating unit
EP^t	Energy prices at time t
E_i^t	Emission volume of i^{th}generating unit at time t

E_{Prod}^{Limit}	Specified limit for the production of emission volume
F_{TC}	Objective cost function of the study
f_{PDF}^{WTG}	Probability distribution function (PDF) of a WTG
f_{Beta}^{PV}	Beta distribution function of a PV
$FVBL_{int}$	Fitness value of the best learner after the initialization stage
$FVWL_{int}$	Fitness value of the worst learner after the initialization stage
$FVBL_{Learn}$	Fitness value of the best learner after the teaching phase
$FVWL_{Learn}$	Fitness value of the worst learner after the teaching phase
I_{ref}	Reference current of a PV at the standard temperature
Inc_j^t	Incentives paid to j^{th} customer at time t
k_t	Coefficient of a PV
k^{WD}, c^{WD}	Shape and scale factor of Weibull distribution function
k_{Pen}^{UE-WTG}	Penalty coefficient for underestimation of a WTG power output
k_{Pen}^{UE-PV}	Penalty coefficient for underestimation of a PV power output
k_{Pen}^{OE-WTG}	Penalty coefficient for overestimation of a WTG power output
k_{Pen}^{OE-PV}	Penalty coefficient for overestimation of a PV power output
LE_i^{Learn}	Learning enthusiasm of i^{th} learner at the learning phase
LE_i^{Te}	Learning enthusiasm of i^{th} learner at the teaching phase
μ_{PV}, σ_{PV}	Mean value and standard deviation of solar irradiance
N_{eq}, N_{ineq}	Number of equality and inequality constraints
N_G	Number of generating units
N_{pop}	Population number at ETLBO
N_{PV}	Number of PV units
N_{POZ}	Number of responsible units for prohibited operating zones
N_{resv}	Number of reserve units responsible for the SRR
N_{WTG}	Number of WTG units
P_i^t	Power output of i^{th} generating unit at time t
$P_i^{resv,t}$	Reserve schedule of i^{th} generating unit at time t
$P_{wind,i}^t$	Schedule of i^{th} WTG at time t
$P_{PV,i}^t$	Schedule of i^{th} PV at time t
$P_{wind,i}^{ava}$	Available power output of i^{th} WTG
P_{PV}^{ava}	Available power output of i^{th} PV
$P_{wind,i}^{exp}$	Expected (forecasted) power of i^{th} WTG
$P_{PV,i}^{exp}$	Expected (forecasted) power of i^{th} PV
P_r^{WTG}	Rated power output of a WTG
P_{PV}^{rated}	Rated power output of a PV
P_i^{Min}, P_i^{Max}	Minimum and maximum power output of i^{th} generating unit
$P_i^{resv,Min}, P_i^{resv,Max}$	Minimum and maximum reserve schedule of i^{th} generating unit
s	Solar radiation at any given time (W/m^2)
T	A time horizon (in this study 24 hours)
T_{amb}	Ambient temperature of a PV
TN_{pop}	Total number of populations
T_{ref}	Reference temperature of a PV
V_i, V_r, V_{Cin} and V_{CO}	Wind speed, rated-speed, cut-in speed, cut-out speed of a WTG
ϖ, ϱ, δ	Tuning parameters of self-adaptive violation handling technique

List of Tables

List of Figures

Acknowledgement

I would like to express my sincere gratitude to my supervisor, Dr. Issa Traoré, for his invaluable guidance and support throughout my master's program. His extensive knowledge and expertise in the field of information security and electrical engineering have been instrumental in enabling me to complete my research and write this report. I am also grateful for his constructive feedback and insightful comments which have helped me to improve the quality of my work.

I would also like to thank Dr. Tao Lu and Dr. Ilamparithi Thirumarai Chelvan for serving on my thesis committee and providing helpful feedback and suggestions.

I am grateful to electrical and computer engineering (ECE) community and graduate studies department for providing me with the opportunity to conduct my research at the University of Victoria, and for all of the resources and support they provided.

Last but not least, I would want to express my gratitude to my friends, family, and especially my wife Judy for their love and continuous support during this journey. This voyage would not have been possible without them.

Dedication

I would like to respectfully dedicate this report to the memory of my late beloved father.

Chapter 1: Prologue

In the evolving energy management landscape, demand response (DR) programs have emerged as critical tools for balancing electricity supply and demand, fostering grid reliability, and facilitating the integration of renewable energy sources. These programs, which incentivize consumers to modify their electricity consumption in response to grid conditions or price signals, have become an integral part of modern electricity markets and smart grids [1].

This chapter delves into the intricate world of DR programs, providing a comprehensive understanding of their origin, structure, types, and the key roles played by various stakeholders. Each section of this chapter is dedicated to answering a fundamental question about DR programs, offering readers detailed and technical insight into this complex yet fascinating subject.

Section 1.1 begins by defining what a demand response program is, laying the foundation for the subsequent sections. Section 1.2 traces the historical development of DR programs, providing context for their current role in energy management. In Section 1.3, we explore the various types of DR programs, highlighting their unique characteristics and applications. Section 1.4 identifies the major participants in DR programs, elucidating their roles and responsibilities. Section 1.5 delves into the structure of DR programs generation resources, offering a glimpse into the diverse sources of electricity that can be modulated through these programs. Finally, Section 1.6 focuses on the pivotal role of consumers in DR programs, outlining their responsibilities and the ways they can contribute to the success of these programs.

By the end of this chapter, readers will have gained a thorough understanding of DR programs, equipping them with the knowledge to navigate this vital aspect of energy management. Whether you are a student, a researcher, a policymaker, or a practitioner in the energy sector, this chapter offers valuable insights into the workings of DR programs, their importance, and their potential for the future of energy systems.

1.1 Understanding Demand Response Programs: A Definition

A DR programs is a strategic energy management initiative designed to adjust the demand for electricity in response to supply conditions. It incentivizes consumers to modify their normal electricity consumption patterns in response to changes in electricity prices or incentives that encourage reduced electricity use during high wholesale market prices or when system reliability is at risk. Playing a crucial role in maintaining the balance between electricity supply and demand, DR programs facilitate the integration of renewable energy sources into the grid and enable consumers to play a more active role in the electricity market. As a key component of modern electricity markets and smart grids, the importance of DR programs is likely to grow as the energy sector continues to evolve [2].

1.2 Historical Development of Demand Response Programs: From Inception to Present

The concept of DR programs originated during the energy crisis in the 1970s. During this period, the United States and many other countries faced significant energy shortages and high prices, leading to the realization that managing energy demand was as important as increasing supply. The initial DR programs were rudimentary and often involved direct load control programs, where utilities would turn off air conditioners or water heaters remotely during peak demand periods [3].

However, the real evolution and sophistication of DR programs began with the deregulation of electricity markets in the late 1990s and early 2000s. Deregulation allowed for the separation of electricity generation, transmission, and distribution and introduced competition into the electricity market. This created an environment where price signals could be used to influence consumer behavior and manage demand, leading to the development of more sophisticated DR programs [4].

The advent of smart grid technology further propelled the evolution of DR programs. Smart grids, with their advanced metering infrastructure and real-time communication capabilities, allow for the implementation of dynamic pricing models and real-time demand response. This has led to the current state of DR programs, where consumers can respond to real-time price signals by adjusting their electricity consumption, thereby contributing to grid stability and efficiency.

1.3 Classification of Demand Response Programs: An Examination of Types and Characteristics

Demand Response (DRP) programs can generally be classified into two broad categories based on the type of incentives they offer: price-based demand response (PBDR) and incentive-based demand response (IBDR) [5].

1) Price-Based Demand Response (PBDR): These programs encourage consumers to reduce their electricity consumption in response to high electricity prices. The price of electricity in these programs varies over time, reflecting the cost of electricity production. Examples of PBDR programs include Time-of-Use (ToU) pricing, Real-Time Pricing (RTP), and Critical Peak Pricing (CPP) [6].
    - Time-of-Use (TOU) Pricing: Electricity prices vary at different times of the day, typically being higher during peak demand periods and lower during off-peak periods.
    - Real-Time Pricing (RTP): Electricity prices are adjusted in real-time based on the current supply and demand conditions.
    - Critical Peak Pricing (CPP): Electricity prices are significantly higher during periods of exceptionally high demand or when the supply is constrained.

2) Incentive-Based Demand Response (IBDR): These programs offer incentives to consumers who agree to reduce their electricity consumption upon request. The incentives can be in the form of direct payments, bill credits, or lower electricity rates. Examples of IBDR programs include Direct Load Control (DLC), Interruptible/Curtailable Service (I/C), and Demand Bidding/Buyback Program (DBP) [7].
   - Direct Load Control (DLC): The utility has the ability to remotely control certain appliances (such as air conditioners or water heaters) in consumers' homes or businesses to reduce electricity consumption during peak periods.
   - Interruptible/Curtailable Service (I/C): Large commercial and industrial customers agree to reduce their electricity consumption upon request in exchange for a reduced electricity rate or other incentives.
   - Demand Bidding/Buyback Program (DBP): Consumers bid to reduce their electricity consumption at certain times in exchange for a payment or bill credit.

These DR programs types provide a flexible framework for managing electricity demand, contributing to grid stability, and promoting efficient use of electricity resources.

1.4 Key Participants in Demand Response Programs: Roles and Responsibilities

The implementation and success of DR programs involve several key participants, each playing a unique role [8, 9]:

- Consumers: These are the end-users of electricity, including residential households, commercial businesses, and industrial facilities. Consumers participate in DR programs by adjusting their electricity usage in response to price signals or incentives.
- Utilities: These are the companies that generate, transmit, and distribute electricity. Utilities often implement DR programs to manage their load, ensure grid stability, and avoid the high costs associated with peak demand periods. They provide incentives or price signals that encourage consumers to adjust their electricity usage.
- Independent System Operators (ISOs) / Regional Transmission Organizations (RTOs): These organizations manage the operation of the electricity market and the transmission grid in a particular region. They use DR programs to balance supply and demand on the grid, especially during periods of peak demand or when there are constraints on the transmission system.
- Aggregators or Demand Response Providers: These are third-party companies that aggregate the demand response capabilities of multiple consumers, particularly small consumers who may not be able to participate in the DR programs on their own. They coordinate the response of these

consumers during a demand response event and often share a portion of the payments or savings with the consumers.

- Regulators: These are government or independent entities that oversee the electricity market and ensure that it operates in a fair, competitive, and reliable manner. Regulators set the rules for DR programs, including how they are implemented and how payments or incentives are distributed.
- Technology Providers: These companies provide the technology needed to implement DR programs, such as smart meters, energy management systems, and communication networks. These technologies enable real-time monitoring and control of electricity usage, which is crucial for the effective operation of DRPs.

1.5 Generation Resources in Demand Response Programs

The generation resources structure of DR programs refers to the various sources of electricity that can be modulated through these programs to balance supply and demand on the grid. This structure is diverse and can include traditional power plants, renewable energy sources, and even the consumers themselves. Here's a brief overview [10-12]:

- Traditional Power Plants: These include coal-fired, natural gas, nuclear, and hydroelectric power plants. While these sources provide the bulk of the electricity supply, their output can be adjusted (within certain limits) in response to demand. However, the ability to modulate output varies by type. For instance, coal and nuclear plants are typically used for base load and are not easily adjusted, while natural gas and hydroelectric plants can be ramped up or down more quickly.
- Renewable Energy Sources: These include wind turbines, solar panels, and other renewable energy technologies. While these sources are environmentally friendly, their output is variable and depends on weather conditions. DR programs can help manage this variability. For instance, during periods of high wind or solar output, consumers can be incentivized to increase their electricity usage to absorb the excess generation.
- Distributed Energy Resources (DERs): These are small-scale power generation or storage technologies (like rooftop solar panels or home batteries) located close to where electricity is used (e.g., at homes or businesses). DERs can participate in DR programs by reducing their demand (i.e., using less electricity from the grid) or by increasing their supply (i.e., generating more electricity and feeding it back into the grid).
- Consumers: In some advanced DR programs, consumers themselves can be considered as part of the generation resources structure. This is particularly true in programs that involve "demand bidding" or "demand buyback" where consumers are paid for agreeing to reduce their electricity usage at times of high demand, effectively acting as "virtual power plants".

- Energy Storage: Energy storage technologies, such as batteries or pumped hydro storage, can store excess electricity during periods of low demand and release it during periods of high demand. They can participate in DR programs by discharging their stored energy into the grid during peak periods.

The specific structure of generation resources in a DR program can vary depending on the characteristics of the local electricity market, the available generation and storage technologies, and the needs and capabilities of the consumers.

1.6 The Role of Consumers in Demand Response Programs: Responsibilities and Contributions

In DR programs, consumers or customers play a pivotal role. Their responsibilities and roles can be outlined as follows [13, 14]:

- Active Participation: Consumers are expected to actively participate in DR programs by responding to signals or incentives from utilities or aggregators. This could involve reducing or shifting their electricity usage during peak demand periods or when electricity prices are high.
- Understanding Pricing Models: Different DR programs have different pricing models, such as Time-of-Use (TOU), Critical Peak Pricing (CPP), or Real-Time Pricing (RTP). Consumers need to understand these models to respond effectively to price signals.
- Investment in Technology: To participate in some types of DR programs, consumers may need to invest in certain technologies, such as smart meters or home energy management systems. These technologies enable real-time monitoring and control of electricity usage, which is crucial for the effective operation of DR programs.
- Communication with Utility or Aggregator: Consumers need to maintain open lines of communication with their utility or aggregator. This can involve providing feedback on the DR program, reporting any issues or concerns, and staying informed about any changes to the program.
- Flexibility: The nature of DR programs requires flexibility from consumers. They may need to adjust their daily routines or operations to reduce or shift their electricity usage at certain times.
- Awareness and Education: Consumers need to be aware of the importance of DR programs in maintaining grid stability and promoting energy efficiency. They should also educate themselves about the specific DR program they are participating in and how they can maximize their benefits from the program.

By fulfilling these roles and responsibilities, consumers contribute significantly to the success of DR programs, helping to ensure grid stability, promote energy efficiency, and potentially save on their electricity bills [15].

Chapter 2: Introduction

2.1 Customer-centric demand response (DR) programs

Customer-centric demand response programs offer a sophisticated approach to managing electricity consumption during periods of high demand or stress on the power grid. By prioritizing customer engagement and empowerment, these programs enable residential and commercial users to actively participate in demand response events, ultimately contributing to a more resilient and efficient electrical system.

Key elements of customer-centric demand response programs include:

1) <u>Effective communication and engagement:</u> Utilizing advanced marketing strategies, user-friendly web portals, and social media platforms, these programs inform and educate customers about demand response, its benefits, and methods of participation.
2) <u>Targeted incentives and dynamic pricing:</u> By offering financial incentives or implementing dynamic pricing models such as time-of-use rates, critical peak pricing, or real-time pricing, customers are encouraged to shift or curtail their energy consumption during peak periods, thereby alleviating grid stress.
3) <u>Smart grid technology integration:</u> The adoption of smart grid technologies, including smart meters, demand management systems, and Internet of Things (IoT) devices, allows customers to monitor and control their energy usage in real-time, enabling more effective participation in demand response events.
4) <u>Flexibility and choice in participation:</u> By providing various opt-in and opt-out options and tailoring participation levels, customer-centric demand response programs become more appealing, fostering increased involvement from a diverse range of customers.
5) <u>Personalized recommendations and feedback:</u> Leveraging data analytics and machine learning algorithms, these programs offer customized energy management advice and real-time feedback on consumption patterns, empowering customers to make informed decisions regarding their participation in demand response events.
6) <u>Collaboration with stakeholders:</u> Establishing partnerships with utilities, regulators, and other stakeholders is essential for the successful implementation and continuous improvement of customer-centric demand response programs.

By focusing on customer needs and preferences while integrating cutting-edge technologies and strategies, customer-centric demand response programs have the potential to significantly reduce peak demand, enhance grid reliability, and facilitate the integration of renewable energy resources into the electricity system.

2.2 Literature Review on Customer-centric DR programs

2.2.1 The Core Concept

A customer-centric demand response program is a program in which customers, such as households or businesses, are incentivized to decrease their energy use during periods of high load demand on the electrical grid. This can be done by providing financial incentives or other rewards for reducing consumption, or by giving customers tools and information to help them better manage their energy use [16]. The incentives offered through a customer-centric demand response program can vary, but they may include things like cash rebates, bill credits, or other financial incentives for reducing energy usage [17].

In general, customer-centric DR programs are designed to consider the preferences and constraints of the customers and to make it easy for them to participate. In contrast, a non-customer-centric demand response program is a program that is primarily focused on reducing peak demand on the electrical grid without considering the preferences and constraints of the customers. In a non-customer-centric demand response program, customers may be provided with limited or no incentives to encourage them to shift their energy usage to non-peak hours. Therefore, the main objective of a non-customer-centric DR program is to reduce peak demand on the electrical grid and may not be as effective in encouraging customer participation.

A thorough literature review on the usage of game theoretic methods in demand response programs has been conducted, where its results show that game theory has been widely used to model and design demand response programs [18]. According to the surveyed literature, various game theoretic methods have been used to model the interactions between customers and utility companies. In the following, we will present the studied game theoretic models on DR programs.

2.2.2 Stackelberg Game: One of the most popular game theoretic methods used in demand response literature is the Stackelberg game. This method models the interactions between the utility company, which acts as the leader, and the customers, who act as the followers [19-21].

2.2.3 non-Cooperative Game: This method models the interactions between customers as they make decisions on their energy consumption independently [22]. The literature has shown that non-cooperative games can be used to design demand response programs that align the incentives of customers and the utility company so that both parties benefit from reduced energy usage during peak demand [23, 24].

2.2.4 Auction Theory Game: This method models the interactions between customers and the utility company as an auction, where customers bid on the amount of energy they want to consume at different prices. Studies using this method have shown that auction theory can be used to design demand response programs that effectively allocate the costs and benefits of demand response among different customers [25, 26].

2.2.5 Mechanism Design (MD) Game: One game theoretic method that has been widely studied in the literature is the Mechanism Design (MD). MD is a branch of game theory that is used to design mechanisms that align the incentives of different agents in a system. In the context of demand response, MD can be used to design mechanisms that align the incentives of customers and the utility company so that both parties benefit from reduced energy usage during peak demand. The literature has shown that MD can be used to design auction-based mechanisms, such as Vickrey-Clarke-Groves (VCG) mechanism, to allocate the costs and benefits of demand response among different customers [27-29].

2.2.6 Cooperative Game Theory: Another game theoretic method that has been widely studied in the literature is the Cooperative Game theory (CGT). CGT is a branch of game theory that studies situations where the agents can form coalitions and make binding agreements. In the context of demand response, CGT can be used to model the interactions between customers as they form coalitions and make agreements to shift their energy consumption [30, 31].

2.2.7 Evolutionary Game Theory: Evolutionary game theory is a method that models the interactions between agents as a dynamic process, where the agents adapt their behavior based on the behavior of others. In the context of demand response, evolutionary game theory can be used to model the interactions between customers as they adapt their energy consumption based on the behavior of others [32, 33].

2.2.8 Bayesian Games: Bayesian games are a type of game theory where agents have uncertain information about the actions or payoffs of other agents. In the context of demand response, Bayesian games can be used to model the interactions between customers and the utility company as they have uncertain information about the actions or payoffs of other agents [34, 35].

2.2.9 Contract Theory: Contract theory is a method that models the interactions between agents as a contract, where the agents make agreements about their actions or payoffs. In the context of demand response, contract theory can be used to model the interactions between customers and utility company as they make agreements about their energy consumption [36, 37].

2.2.10 Differential Games: Differential games are a type of game theory where the agents control the evolution of a dynamic system, such as a heat engine or an electric grid. In the context of demand response, differential games can be used to model the interactions between customers and the utility company as they control the evolution of the electric grid [38, 39].

2.2.11 Repeated Games: Repeated games are a type of game theory where the same game is played multiple times, allowing the agents to learn from their past actions and adapt their behavior. In the context of demand response, repeated games can be used to model the interactions between customers and the utility company as they learn from their past actions and adapt their behavior to reduce their electricity costs [40, 41].

2.2.12 Mean Field Games: Mean field games are a type of game theory where the agents interact with a large number of other agents, and their behavior is influenced by the behavior of the population as a whole [42, 43].

2.2.13 Reinforcement Learning: A game theoretic method that has been recently studied in the literature is Reinforcement Learning (RL). RL is a method of machine learning that can be used to model the interactions between the agents in a dynamic system. In the context of demand response, RL can be used to model the interactions between customers and the utility company as they learn from their past actions and adapt their behavior to reduce their electricity costs [44-46].

In all the above-mentioned game theoretic methods, the studies have shown that these methods can be used to design demand response programs that encourage customers to shift their energy usage to non-peak hours, while also considering the customers' preferences and the network constraints [4, 47-49].

However, a comprehensive review of the literature reveals a gap in this field. While there are studies that consider customer benefits and flexibility in the context of demand response programs, none have explicitly combined these customer-centric attributes in their formulations. For instance, Koolen et al. [50] discuss the role of home energy management systems in enhancing demand flexibility, but do not explicitly combine customer benefits and flexibility. Similarly, Sharifi et al. [51] propose a market-oriented demand response model that encourages residential consumers to adjust their consumption patterns to maximize benefits, but this model focuses on the consumers' response to price signals rather than a combination of their benefits and flexibility. Further, Dadkhah et al. [52] propose a security-constrained structure for power systems that enhances flexibility through the coordination of generation and demand sides. However, their focus is on the system's adaptability to contingencies and wind power variability, not on combining customer benefits and flexibility. Azimian et al. [53] discuss the use of demand response programs to enhance the resilience of energy systems, proposing a probabilistic optimization model for networked multi-carrier microgrids that integrates flexibility potentials into the microgrids. Yet, their study is centered on improving system resilience rather than combining customer benefits and flexibility. This lack of research on methods that integrate customer benefits and flexibility in a customer-centric manner in DR programs underscores the need for further exploration in this area.

2.3 Benefits to Both Parties

Customer-centric demand response programs can bring multiple benefits to both utilities and customers [54, 55]:

Benefits to Utilities:

1) Load balancing: DR programs can help utilities balance load on the grid and avoid overloading, ensuring a stable power supply.
2) Cost savings: By reducing peak demand, DR programs can lower energy production and distribution costs for utilities.
3) Improved reliability: DR programs have the ability to enhance the reliability of the power grid by reducing the likelihood of blackouts and brownouts.
4) Better grid management: DR programs can provide real-time information on demand and usage patterns, allowing for more efficient grid management.
5) Increased renewable energy integration: DR programs can facilitate the integration of renewable energy sources into the grid, helping utilities meet renewable energy goals.

Benefits to Customers:

1) Cost savings: By reducing peak demand, DR programs can lower energy bills for customers.
2) Increased energy efficiency: DR programs can encourage customers to use energy more efficiently, reducing waste and saving money.
3) Consumer engagement: DR programs can empower customers to take an active role in managing their energy consumption and costs, increasing engagement and satisfaction.

2.4 Statement of Contribution

The novel contributions of this research as compared to the discussed literature can be expressed as follows:

- A game-theoretic, customer-centric demand response (CC-GTDR) framework is devised to capture intricate interactions between utilities and consumers in a liberalized market context. The CC-GTDR approach exceptionally integrates incentive-based and price-based demand response programs, emphasizing consumer benefits and choice flexibility. This formulation fosters a mutually advantageous scenario for all market players, particularly accentuating customer rights within a monopolistic market setting.
- A fuzzy analytic hierarchy process incorporating non-linear programming (FAHP-NLP) is devised and applied to determine the optimal weights for the study's multi-criteria objective function. The proposed FAHP-NLP method prioritizes the CC-GTDR objectives in alignment with the grid operator's viewpoints.

- A sequential hybrid algorithm, combining an enthusiasm-aided teaching and learning-based optimization (EaTLBO) with an enhanced particle swarm optimization (EPSO), is proposed for addressing the multi-criteria non-convex objective function formulation.

2.5 Report Organization

The structure of the report is as follows: The "Nomenclature" section defines all acronyms and variables. Chapter 1 provides a detailed background of this research, where Chapter 2 offers an extensive review of pertinent literature. Chapters 3 and 4 present the concepts and mathematical formulations of the study. Chapter 5 outlines the development of the proposed hybrid algorithm (EaTLBO-EPSO) and its weighting method in detail. A thorough analysis of the results and their related discussions are provided in Chapter 6, while Chapter 7 concludes with a summary of the study’s key findings.

Chapter 3: Problem Formulation

3.1 Dynamic combined economic and emission dispatch (DCEED)

The multi-criteria dynamic combined economic and emission (DCEED) formulation aims to minimize costs (generation fuel, emission production, reserve, socio-economic, and RES) and maximize expected profit, social welfare, and DRP participation. Utility revenues stem from electricity sales to residential, commercial and industrial consumers, considering bilateral contracts. In the deregulated power market's short-term dynamic generation dispatch, cost-related criteria weights are assigned by the market operator (MO). This leads to the study's primary objective formulation:

$$\begin{aligned} Min(F_{TC}) = {} & w^{Gen}\left(\sum_{t=1}^{T}\sum_{i=1}^{N_G} C_i^{Gen,t}(P_i^t)\right) + w^{Resv}\left(\sum_{t=1}^{T}\sum_{i=1}^{N_{resv}} C_i^{resv,t}\left(P_i^{resv,t}\right)\right) \\ & + w^{Emi}\left(\sum_{t=1}^{T}\sum_{i=1}^{N_G} C_i^{emi,t}(P_i^t)\right) + w^{CSEI}\left(\sum_{t=1}^{T}\sum_{i=1}^{N_G}\left(CSEI(P_i^t)\right)\right) \\ & + w^{REN}\left(\sum_{t=1}^{T}\sum_{i=1}^{N_{WTG}} C_i^{WTG,t}\left(P_{wind,i}^t\right) + \sum_{t=1}^{T}\sum_{i=1}^{N_{PV}} C_i^{PV,t}\left(P_{PV,i}^t\right)\right) \\ & + w^{GTDR}\left(\sum_{t=1}^{T}\sum_{j=1}^{N_j}\left(Inc_j^t - \lambda_j^t \times L_{curb,j}^t\right)\right) \end{aligned} \tag{1}$$

In Eq. 1, F_{TC} is the objective cost function of the study; $C_i^{Gen,t}, C_i^{resv,t}, C_i^{emi,t}, C_i^{WTG,t}$ and $C_i^{PV,t}$ are cost of thermal unit i at time t, cost of the generating reserve for unit i at time t, cost of emission produced by unit i at time t, cost of power generated by wind turbine i at time t, and cost of power generated by PV unit i at time t, respectively; $P_i^t, P_i^{resv,t}, P_{wind,i}^t$ and $P_{PV,i}^t$ are generated power by thermal generating unit i at time t, reserve schedule of unit i at time t, schedule of wind turbine unit i at time t, schedule of PV unit i at time t, respectively; $w^{Gen}, w^{Resv}, w^{Emi}, w^{CSEI}, w^{REN}$ and w^{GTDR} are the weighting factors for thermal generation, reserve, emission, renewable resources, and game-theoretic demand response, respectively; Inc_j^t is the amount of incentive paid to customer j at time t; λ_j^t is the locational marginal price that is paid to customer j at time t; $L_{curb,j}^t$ is the curbed load of the customer j at time t.

The Eq. 1 encapsulates the primary objective function driving this study, encompassing six distinct cost functions. These include the cost of power generation, the cost associated with maintaining spinning reserves, emission-related costs, socioeconomic interruption costs, the cost of utilizing renewable resources, and the expenses tied to demand response programs. Each of these cost functions is assigned a unique criterion weight. This allocation aids the MO in pinpointing the optimal solution that aligns with the distinct characteristics of a deregulated electricity market, thereby facilitating a more efficient and targeted approach to energy management.

3.2 Cost of generation

The objective of minimizing fuel costs for all active generators can be described in more detail as the process of reducing the generation costs associated with thermal units while considering the impact of their valve-point loading effects (VPLEs):

$$\sum_{t=1}^{T}\sum_{i=1}^{N_G} C_i^{Gen,t}(P_i^t) = \sum_{t=1}^{T}\sum_{i=1}^{N_G}(a_i + b_i P_i^t + c_i (P_i^t)^2) + \left|d_i \times \sin(e_i \times (P_i^{Min} - P_i^t))\right| \tag{2}$$

In Eq. 2, a_i, b_i, c_i, d_i and e_i are cost coefficient of generating unit i, respectively; P_i^{Min} is the minimum schedule of generator i.

3.3 Cost of reserve

To run an electrical grid with the utmost peace of mind in the event of a contingency, the study has implemented and investigated the following procedures for two purposes; first, to give flexible options to the MO for management of the system reserve requirement, and second, to reduce the reserve costs while maintaining the system reliability at an apt level.

1) The units with prohibited operating zones (POZs) shall not participate in the system reserve requirement level (RRL) calculations as their power output is constrained due to the generating units' physical limitations, and they will also cause a significant deviation from the existing dispatch plan.
2) The non-POZ units must be held accountable for the satisfaction of the system RRL.
3) The RRL will be defined and allocated among the online units based on the MO experiences and the empirical analysis.
    - In this case, the cumulative amount of the regulating reserve and contingency reserve will be dispatched between all the designated units.
4) The system RRL will be dispatched according to the judgment of the utilized optimization algorithm.
    - In this instance, an optimization algorithm has been designed to determine the share of each unit in the fulfillment of the reserve requirement.

The main criterion for dispatching of the reserve schedules among the available generators is based on their reserve cost function that is given as:

$$\sum_{t=1}^{T}\sum_{i=1}^{N_{resv}} C_i^{resv,t}(P_i^{resv,t}) = \left(a_i^{resv} + b_i^{resv}P_i^{resv,t} + c_i^{resv}\left(P_i^{resv,t}\right)^2\right) + \left|d_i^{resv} \times \sin(e_i^{resv} \times (P_i^{resv,Min} - P_i^{resv,t}))\right| \quad (3)$$

In Eq. 3, $a_i^{resv}, b_i^{resv}, c_i^{resv}, d_i^{resv}$ and e_i^{resv} are the reserve cost coefficients of generating unit i, and $P_i^{resv,Min}$ is the minimum reserve schedule of generator i.

3.4 Emission cost function

In this study, a flexible emission constraint strategy is formulated to decrease the production of multiple pollutant gases, thereby ensuring compliance with the Clean Air Act Amendment's environmental regulations [56, 57]. To fully assess the cost of pollutant emissions from thermal power generators, Eq. 4 provides a combined cost calculation. This calculation includes both the expense of filtering emissions and the potential penalty costs linked to the emission of carbon dioxide (CO_2), sulfur oxide (SO_2), and nitrogen oxide (NO_X). This unified approach thus offers a comprehensive financial analysis of the environmental implications associated with thermal power generation. Therefore, the formulation is presented as [57]:

$$\begin{aligned}\sum_{t=1}^{T}\sum_{i=1}^{N_G} E_i{}^t(P_i^t) &= \sum_{t=1}^{T}\sum_{i=1}^{N_G} E_i^{CO_2,t}(P_i^t) + \sum_{t=1}^{T}\sum_{i=1}^{N_G} E_i^{SO_2,t}(P_i^t) + \sum_{t=1}^{T}\sum_{i=1}^{N_G} E_i^{NO_x,t}(P_i^t) \\ &= \sum_{t=1}^{T}\sum_{i=1}^{N_G}\left(\alpha_i^{CO_2} + \beta_i^{CO_2}P_i^t + \gamma_i^{CO_2}(P_i^t)^2\right) + \eta_i^{CO_2}\exp\left(\delta_i^{CO_2}P_i^t\right) \\ &+ \sum_{t=1}^{T}\sum_{i=1}^{N_G}\left(\alpha_i^{SO_2} + \beta_i^{SO_2}P_i^t + \gamma_i^{SO_2}(P_i^t)^2\right) + \eta_i^{SO_2}\exp\left(\delta_i^{SO_2}P_i^t\right) \\ &+ \sum_{t=1}^{T}\sum_{i=1}^{N_G}\left(\alpha_i^{NO_x} + \beta_i^{NO_x}P_i^t + \gamma_i^{NO_x}(P_i^t)^2\right) + \eta_i^{NO_x}\exp\left(\delta_i^{NO_x}P_i^t\right)\end{aligned} \quad (4)$$

To consider the effects of multi-pollutant gas emissions on total production costs, these emissions must be represented in terms of their associated penalty costs.

$$\sum_{t=1}^{T}\sum_{i=1}^{N_G} C_i^{emi,t}(P_i^t) = k^{CO_2}\left(\sum_{t=1}^{T}\sum_{i=1}^{N_G} E_i^{CO_2,t}(P_i^t)\right) + k^{SO_2}\left(\sum_{t=1}^{T}\sum_{i=1}^{N_G} E_i^{SO_2,t}(P_i^t)\right) + k^{NO_x}\left(\sum_{t=1}^{T}\sum_{i=1}^{N_G} E_i^{NO_x,t}(P_i^t)\right) \quad (5)$$

In Eqs. 4 and 5, $E_i^{CO_2,t}, E_i^{SO_2,t}$ and $E_i^{NO_x,t}$ are carbon-dioxide emission produced by unit i at time t, Sulphur-dioxide emission produced by unit i at time t, Nitrogen-oxide emission produced by unit i at time t, respectively; k^{CO_2}, k^{SO_2} are k^{NO_x} are the cost weightings of carbon-dioxide, Sulphur-dioxide and Nitrogen-oxide during the optimization process, respectively; $\alpha_i^{CO_2}, \beta_i^{CO_2}, \gamma_i^{CO_2}, \eta_i^{CO_2}$ and $\delta_i^{CO_2}$ are CO_2 cost coefficients associated with unit i, respectively.

3.5 The cost of socio-economic interruption (CSEI)

The socio-economic cost of generation supply interruption, representing losses for different load types (in this study referred to the residential consumers) is the related cost of load shedding [58]. Since forecasting the probability of a supply outage during the implementation of a generation dispatch plan is highly challenging, only an estimated cost of interruptions can be determined. Accordingly, Eq. 6 and Eq.7 represent the calculations for the expected energy not served (EENS) and the cost of socio-economic interruption (CSEI) across the entire power system, respectively. These equations provide an in-depth analysis of the potential operational disruptions and their associated socio-economic costs in the context of power system energy management.

$$EENS(P_i^t) = \sum_{t=1}^{T}\sum_{i=1}^{N_G}(FOR_i \times h \times P_i^t) \tag{6}$$

$$\sum_{t=1}^{T}\sum_{i=1}^{N_G} CSEI(P_i^t) = \sum_{t=1}^{T}\sum_{i=1}^{N_G}(EENS(P_i^t) \times VOLL\ ) \tag{7}$$

In Eqs. 6 and 7, FOR_i is the forced outage rate of generator i; h is the hour; $VOLL$ is the value of the lost load, $EENS$ is the expected energy not served.

3.6 Cost function for wind energy

The comprehensive operating cost of wind turbine generators, accounting for the levelized cost of wind energy (LCOWE), penalty cost for underestimating available wind power (UAWP), and overestimating reserve requirement levels (ORRL) after wind energy integration, can be determined using the subsequent formulation:

$$\begin{aligned}\sum_{t=1}^{T}\sum_{i=1}^{N_{WTG}} C_i^{WTG,t}\left(P_{wind,i}^t\right) = \\ = \overbrace{\sum_{i=1}^{N_{WTG}} C_{Gen,i}^{WTG}(P_{wind,i}^t)}^{LCOWE\ (I)} + \overbrace{\sum_{i=1}^{N_{WTG}} C_{Pen,i}^{AWP}[(P_{wind,i}^{ava})^t - (P_{wind,i}^{exp})^t]}^{UAWP\ (II)} \\ + \overbrace{\sum_{i=1}^{N_{WTG}} C_{Pen,i}^{SR-WTG}[(P_{wind,i}^{exp})^t - (P_{wind,i}^{ava})^t]}^{ORRL(III)}\end{aligned} \tag{8}$$

In Eq. 8, $P_{wind,i}^t$, $P_{wind,i}^{ava}$ and $P_{wind,i}^{exp}$ are generating schedule of wind turbine generator i at time t, available power output of wind turbine generator i at time t, expected or forecasted power output of wind turbine generator generating schedule of wind turbine generator i at time t, respectively; $C_i^{WTG,t}$, $C_{Gen,i}^{WTG}$, $C_{Pen,i}^{AWP}$ and $C_{Pen,i}^{SR-WTG}$ are total generation cost of i^{th} wind turbine generator at time t, generation cost of i^{th} wind turbine generator, underestimation cost of available wind power of i^{th} wind turbine generator, overestimation cost of spinning reserve requirement for i^{th} wind turbine generator, respectively.

3.7 Cost function for Photovoltaic (PV) energy

The combined operating cost of photovoltaic panels taking into account levelized cost of PV energy (LCOPVE), penalty cost due to underestimation of available PV energy (UAPVE) and overestimation of the reserve requirement level (ORRL) after incorporation of wind energy can be defined as:

$$\sum_{t=1}^{T}\sum_{i=1}^{N_{PV}} C_i^{PV,t}(P_{PV,i}^{t}) = \overbrace{\sum_{i=1}^{N_{PV}} C_{Gen,i}^{PV}(P_{out,i}^{PV,t})}^{LCOPVE\ (I)} + \overbrace{\sum_{i=1}^{N_{PV}} C_{Pen,i}^{APVP}[(P_{PV,i}^{ava})^t - (P_{PV,i}^{exp})^t]}^{UAPVE\ (II)} + \overbrace{\sum_{i=1}^{N_{PV}} C_{Pen,i}^{SR-PV}[(P_{PV,i}^{exp})^t - (P_{PV,i}^{ava})^t]}^{ORRL\ (III)} \tag{9}$$

In Eq. 9, $P_{PV,i}^{t}$, $P_{PV,i}^{ava}$ and $P_{PV,i}^{exp}$ are Schedule of i^{th} PV at time t, Available power output of i^{th} PV, Expected (forecasted) power of i^{th} PV, respectively; $C_i^{PV,t}$, $C_{Gen,i}^{PV}$, $C_{Pen,i}^{APVP}$ and $C_{Pen,i}^{SR-PV}$ are total generation cost of i^{th} PV at time t, generation cost of i^{th} PV, underestimation cost of available solar power of i^{th} PV, overestimation cost of spinning reserve requirement for i^{th} PV, respectively.

3.8 A self-adaptive power violation constraint management approach (SaPVCMA)

So far, we have explained the study objective function and its related cost functions. However, study objective function (Eq. 1) is subjected to several constraints such as physical, operational, and environmental. Thus, a thorough power violation constraint framework has been established using a self-adaptive penalty management approach to guarantee the correctness of the EaTLBO-EPSO's supplied solutions. The devised SaPVCMA keeps track of two different forms of equality constraints as well as seven distinct types of inequality constraints. In this study, the equality constraints are indexed as h_{eq}, where the inequality constraints are termed as g_{ineq}.

Power balance violation (PBV): The PBV equation is a crucial instrument in power systems analysis that illustrates the principle of energy conservation. In essence, it quantifies the discrepancy between the total power injected into the system and the total power consumed plus transmission losses. A non-zero PBV implies a power imbalance, necessitating intervention to prevent system instability, while a zero value indicates an ideal state of power equilibrium. Thus, PBV is central to optimizing power system operation and maintaining stability.

$$h_{(1)}^{PBV} = Max\left(abs\left(1 - \frac{\left(\sum_{i=1}^{N_G} P_i^t\right) - P_{Loss}^t}{\left(P_D^t - \sum_{j=1}^{J} L_{curb,j}^t\right)}\right), 0\right) \tag{10}$$

In Eq. 10, P_L^t is the power losses at the time t; P_L^t is the load demand at the time t and $L_{curb,j}^t$ is the curbed load at the time t for customer j.

<u>*Reserve balance violation (RBV):*</u> The RBV equation is a fundamental analytical tool in power systems management. It assesses the imbalance between the total power reserve available in the system and the required reserve capacity that needs to be maintained for grid reliability. A non-zero RBV signifies a shortfall or surplus in reserve capacity, requiring operational adjustments, whereas a zero RBV indicates an ideal balance, where the available reserve precisely meets the required reserve capacity. Hence, RBV plays an essential role in ensuring uninterrupted power supply and mitigating risks of unforeseen grid disturbances.

$$h_{(2)}^{RBV} = Max\left(abs\left(1 - \frac{\left(\sum_{i=1}^{N_{resv}} P_i^{resv,t}\right)}{\left(SRR_{Con}^t + SRR_{Reg}^t\right)}\right), 0\right) \tag{11}$$

in which

$$SRR_{Con}^t = \omega_{LOU} \times P_{LOU}^{t,Exp} + \left(\omega_{VGRs} \times \left(P_{WTG}^{t,Exp} + P_{PVG}^{t,Exp}\right)\right) \tag{12}$$

$$SRR_{Reg}^t = \psi \times \sqrt{\frac{\left(\omega_{P_D} \times P_D^t\right)^2}{3} + \delta_{ST}^{Wind}(P_{WTG}^t) + \delta_{ST}^{PVG}(P_{PVG}^t)} \tag{13}$$

In Eqs. 11, 12 and 13, SRR_{Con}^t is the contingency category of spinning reserve requirement at time t; SRR_{Reg}^t is the regulating category of spinning reserve requirement at time t; ω_{LOU} is the weighting factor for the largest online unit; $P_{LOU}^{t,Exp}$ is the expected power schedule of the largest online unit at time t; ω_{VGRs} is the weighting factor for the variable generations; $P_{WTG}^{t,Exp}$ is the expected total power output of wind farms at time t; $P_{PVG}^{t,Exp}$ is the expected total power output of PV farms at time t; ψ is the weighting factor of the spinning reserve requirement; ω_{P_D} is the weighting factor of the power demand; δ_{ST}^{Wind} is the power output standard deviation of wind farms; δ_{ST}^{PVG} is the power output standard deviation of PV farms.

<u>*Power constraint violation (PCV):*</u> The PCV equation is an essential metric in power system studies that quantifies the extent to which power generation or transmission exceeds or falls short of its specified limits. A non-zero PCV indicates a violation of the prescribed power bounds, signaling potential risks to grid stability or equipment safety, while a zero PCV implies that all power constraints are being adhered to. Therefore, monitoring and managing PCV is critical to maintaining the safe and efficient operation of power systems.

$$g_{(1)}^{PCV} = \sum_{i=1}^{N_G}\left[\max(P_i^t - P_i^{Max}, 0) + \max\left(P_i^{Min} - P_i^t, 0\right)\right] \tag{14}$$

In Eq. 14, P_i^{Max} is the maximum limit of generator i.

Ramp-rate limit violation (RRLV): The RRLV equation is a pivotal measure in power system management, denoting the degree to which a power source's change in output violates its predefined ramp-rate limits. A non-zero RRLV signifies that the rate of power output change exceeds or undershoots the allowed rate, hinting at potential system instability or equipment stress. In contrast, a zero RRLV suggests strict adherence to ramp-rate constraints, contributing to the seamless functioning of power systems. Thus, RRLV plays a key role in ensuring smooth transitions in power generation and preserving system reliability.

$$g_{(2)}^{RRLV} = \sum_{i=1}^{N_G}[\max(P_i^t - P_i^0 - UR_i, 0) + \max(P_i^0 - P_i^t - DR_i, 0)] \tag{15}$$

In Eq. 15, P_i^0 is the initial power schedule of generating unit i; UR_i is the upward ramping reserve of generating unit i; DR_i is the downward ramping reserve of generating unit i.

Prohibited operating zones violation (POZV): The POZV equation is a key metric in power system management, quantifying the extent to which a unit's operation falls within the prohibited operating zones. These zones typically represent conditions of unstable operation or limitations due to mechanical or thermal constraints. A non-zero POZV signifies operation within these unfavorable zones, posing risks to system stability and equipment integrity. On the other hand, a zero POZV indicates operation within permissible parameters, ensuring optimal system performance and equipment safety. Therefore, monitoring and minimizing POZV is essential to maintain system reliability and prevent costly equipment damage.

$$g_{(3)}^{POZV} = \sum_{i=1}^{N_G}\sum_{j=1}^{N_{POZ}}\left[\min\left(max\left(P_i^t - P_{i,j}^L, 0\right), max\left(P_{i,j}^U - P_i^t, 0\right)\right)\right] \tag{16}$$

In Eq. 16, $P_{i,j}^L$ is the POZ lower bound of unit i zone j; $P_{i,j}^U$ is the POZ upper bound of unit i zone j.

Reserve constraint violation (RCV): The RCV equations are significant tools in power system management, signifying the degree to which the system's available reserves infringe upon the predefined reserve constraints. These constraints typically account for uncertainty and potential system disturbances, providing a safety buffer. A non-zero RCV indicates that the available reserves are inadequate or excessively surpassing the specified constraints, posing challenges for grid reliability and efficient resource management. Conversely, a zero RCV implies that reserve levels are within the defined limits, contributing to the resilient and economical operation of power systems. Therefore, RCV plays a vital role in maintaining system robustness and managing unforeseen fluctuations in power demand or supply.

$$g_{(4)}^{RCV_{(1)}} = abs\left(\min\left(\sum_{i=1}^{N_G} P_i^{Max} - (P_D^t + P_{Loss}^t + SRR_{Con}^t), 0\right)\right) \tag{17}$$

$$g_{(5)}^{RCV_{(2)}} = abs\left(\min\left(\sum_{i=1}^{N_G} \left(Min(P_i^{Max} - P_i^t, UR_i^t)\right) - (SRR_{Con}^t), 0\right)\right) \tag{18}$$

$$g_{(6)}^{RCV_{(3)}} = abs\left(\min\left(\sum_{i=1}^{N_G} \left(Min\left(P_i^{Max} - P_i^t, UR_i^{t,10\,min}\right)\right) - \left(SRR_{Reg}^t\right), 0\right)\right) \tag{19}$$

<u>*Emission volume constraint (EVC):*</u> The EVC equation is a key instrument in environmentally conscious power system operations. It quantifies the extent to which the greenhouse gas emissions of a power system breach the set regulatory or environmental constraints. A non-zero EVC indicates that the system's emissions surpass the permissible limits, thereby signaling a violation of environmental regulations and potential repercussions. Conversely, a zero EVC suggests adherence to emission constraints, underscoring the system's environmental compliance. Therefore, tracking and managing EVC is essential in achieving sustainable power system operation and contributing to broader environmental objectives.

$$g_{(7)}^{EVC} = \max\left(\sum_{t=1}^{T}\sum_{i=1}^{N_G} E_i{}^t(P_i^t) - E_{Prod}^{Limit}, 0\right) \tag{20}$$

In Eq. 20, $E_i{}^t$ is the emission volume of i^{th}generating unit at time t; E_{Prod}^{Limit} is the specified limit for the production of emission volume.

The SaPVCMA can be characterized by employing a dynamic violation handling method that adaptively determines the values of two penalty weighting factors (PF_1 and PF_2) for the considered constraints.

$$SaPVCMA = \left[PF_1 \times \left(\sum_{eq=1}^{N_{eq}} h_{eq}\right) + PF_2 \times \left(\sum_{ineq=1}^{N_{ineq}} g_{ineq}\right)\right] \tag{21}$$

$$PF_1 = PF_2 = \left(\frac{MaxIter}{Iter}\right) \times \sqrt{Iter} \times \varpi \times \varrho^{\delta} \tag{22}$$

$$if \begin{cases} \varrho \le 1 \rightarrow \quad \varpi = 10{,}000 \rightarrow \quad \delta = 0.1 \\ \varrho \le 0.01 \rightarrow \quad \varpi = 1000 \rightarrow \quad \delta = 0.02 \\ \varrho \le 0.001 \rightarrow \quad \varpi = 500 \rightarrow \quad \delta = 0.003 \\ \varrho \le 0.0001 \rightarrow \varpi = 100 \rightarrow \delta = 0.0004 \end{cases} \tag{23}$$

In Eqs. 21, 22 and 23, h_{eq} is the set of equality constraints; g_{ineq} is the set of inequality constraints; PF_1 and PF_2 are the first and second penalty factors, respectively; $MaxIter$ is the maximum number of iterations during the optimization process; $Iter$ is the number of the current iteration; ϖ, ϱ and δ are the tuning parameters of self-adaptive violation handling technique.

If the SaPVCMA value is zero, all constraints were preserved throughout the optimization process; conversely, any non-zero value indicates a constraint violation. To achieve the best solution, the EaTLBO-EPSO attempts to minimize the Eq.1 plus SaPVCMa that includes all the required constraints ($OF_{min} = F_{TC} + SaPVCHT$).

Chapter 4: Customer-centric game theory-based demand response (CC-GTDR)

Demand response programs involve shifts in customer consumption patterns due to factors such as market price fluctuations, incentives to reduce usage during high prices, or system reliability threats from unforeseen events. In a monopolistic electric utility context, these programs are considered beneficial for power system efficiency, reliability, and resiliency. These benefits manifest as reductions in operating expenses and emissions of harmful gases.

A crucial criterion for utilities implementing demand response programs is offering incentives surpassing customer outage costs. Based on agreements between utilities and customers, incentives may include monetary rewards or reduced power rates. Customers can specify their willingness to curtail power usage and announce varying participation factors based on operation times, termed as time-of-use participation factors (ToU-PF) in this study. The proposed demand response program comprises three essential conditions:

- Customers should be divided into different groups based on the amount of their load levels and their willingness to engage in demand response plans. The term willingness is interpreted as ToU-PF which in this case further enables the utilities to adhere to the customers' rights in the deregulated power market environments.
- The utility's capability in the exact evaluation of customers' outage costs for inclusion of reasonable compensation payments to customers.
- The ability of utility in the inclusion of customers' locational marginal pricing (LMPs) into demand management contracts.

4.1 Customer benefit function in the basic GTDR

In the basic form of the GTDR, the U_j represents the function that defines the customers' benefit; Inc_j is the incentives that must be paid to the customers; K_1 and K_2 are the customers' cost coefficients for determining the cost of outages; θ_j represents the customers' participation factor in joining DR program (value of θ_j is within 0 to 1; in which the 0 shows no interest in DRP participation and 1 expresses the highest interest) and $L_{curb,j}$ is the amount of load that will be curbed by the customer j. For all the customers, it is only logical to participate in GTDR, if U_j is greater than or equal to zero.

$$U_j = Inc_j - \left(K_1 L_{curb,j}^2 + K_2 L_{curb,j} - K_2 L_{curb,j} \theta_j\right), \quad for\ j = 1, \dots, j \tag{24}$$

4.2 Utility benefit function in the basic GTDR

In the basic form of the GTDR, the U_0 represents the function that determines the utility benefit and λ_j is the power interruptibility value for the customer j.

$$U_0 = \sum_{j=1}^{J} (\lambda_j L_{curb,j} - Inc_j) \tag{25}$$

4.3 Inserting demand management contracts into customer-centric GTDR

The GTDR's primary goal is to maximize the expected utility gains using the formula:

$$max \sum_{t=1}^{T} \sum_{j=1}^{J} [\lambda_j^t L_{curb,j}^t - Inc_j^t] \tag{26}$$

Subject to

$$\sum_{t=1}^{T} \left(Inc_j^t - \left(K_{1,j}^t \left(L_{curb,j}^t \right)^2 + K_{2,j}^t L_{curb,j}^t - K_{2,j}^t L_{curb,j}^t \theta_j^t \right) \right) \geq 0 \,, \;\; for\; j = 1, \dots , j \tag{27}$$

The constraint presented in Eq. 27 is called the individual rationality constraint, ensuring customer incentives exceed outage costs and encouraging participation in GTDR. The superscript t has been added to the customers' outage costs coefficients ($K_{1,j}^t$ and $K_{2,j}^t$) as well as the customers' participation factor (θ_j^t) to demonstrate three ideas: i) to display different pricing levels based on load demand behavior throughout a day, ii) to mimic ToU-PF prices in a deregulated power market environment, and iii) to show different customers' participation factors with respect to the time of GTDR implementation. It is worth noting that in all prior studies, either the customer outage costs were not addressed at all, or they were only mentioned as a constant figure that doesn't represent a fair situation when load demand varies. To establish a customer-centric GTDR program within a utility environment, we assigned distinct outage costs and participation factors to each customer, dependent on their load demand capacity and operational hours. Table 4.1 illustrates the proposed customer-centric attributes:

Table 4.1: Concept of customer-centric attributes

Peak		***Partial-Peak***		***Off-Peak***	
$K_{1,j}^t, K_{2,j}^t$	High Value	$K_{1,j}^t, K_{2,j}^t$	Medium Value	$K_{1,j}^t, K_{2,j}^t$	Low Value
θ_j^t	Low Value	θ_j^t	Medium Value	θ_j^t	High Value

The incentive compatibility requirement, Eq. (28) ensures that consumers are paid based on their level of engagement in the GTDR.

$$\sum_{t=1}^{T}\left(Inc_j^t-\left(K_{1,j}^t\left(L_{curb,j}^t\right)^2+K_{2,j}^tL_{curb,j}^t-K_{2,j}^tL_{curb,j}^t\theta_j^t\right)\right) \geq \sum_{t=1}^{T}\left(Inc_{j-1}^t-\left(K_{1,j-1}^t\left(L_{curb,j-1}^t\right)^2+K_{2,j-1}^tL_{curb,j-1}^t-K_{2,j-1}^tL_{curb,j-1}^t\theta_{j-1}^t\right)\right),\ for\ j = 2,\dots,j \tag{28}$$

$$\sum_{t=1}^{T}\sum_{j=1}^{J}Inc_j^t \leq \sum_{t=1}^{T}UB^t \tag{29}$$

where UB^t represents the utility budget for every operation hour of a day.

The utility budget constraint (Eq. 29) ensures that the sum of incentives offered to customers for reducing their loads does not exceed the authorized GTDR budget for the utility. We developed a novel payment allocation method for determining the total incentive expenditures for each operating hour based on the ratio of the load at that hour to the overall load demand. These ratios are then multiplied by the total utility budget to compute the maximum hourly customer incentives. This establishes the hourly utility budget.

$$\sum_{t=1}^{T}L_{curb,j}^t \leq \sum_{t=1}^{T}CM_j^t \quad for\ j = 1,\dots,J \tag{30}$$

where the CM_j^t denotes the maximum hourly limit of interruptible load for customer j.

The consumer hourly interruptibility restriction (Eq. 30) limits load reduction to what customers have declared. Hourly CM_j^t is computed by multiplying hourly load ratios with each customer's daily limit of interruptible load. This determines the maximum load reduction per customer per hour, enabling precise GTDR limitations for each hour. Additionally, total hourly interruptible load for all customers should not exceed 12% of the total hourly load demand to prevent overburdening of critical loads. The profit-based DCEED (PBDCEED) can be formulated mathematically in deregulated power markets.

$$PBDCEED_{max} = \sum_{t=1}^{T}\sum_{i=1}^{N_G}\left(\left(EP^t * (P_i^t)\right)-\left(C_i^{Gen,t}(P_i^t)\right)\right) \tag{31}$$

4.4 Profit and load performance evaluation

Four load performance indexes were used to evaluate the effectiveness of various pricing strategies in enhancing GTDR participation and load demand characteristics. The studied load indexes are total load reduction (TLR), peak load reduction (PLR), peak-to-average ratio (PAR), and peak-to-valley (PtV).

$$TLR = \left(\frac{Load_{Total}^{New} - Load_{Total}^{Old}}{Load_{Total}^{Old}}\right) \times 100 \tag{32}$$

$$PLR = \left(\frac{Load_{Peak}^{New} - Load_{Peak}^{Old}}{Load_{Peak}^{Old}}\right) \times 100 \tag{33}$$

$$PAR = \left(\frac{\max\limits_{t \in T} \sum_{i=1}^{N} D_i(t)}{\frac{1}{T} \times \sum_{i=1}^{N} D_i\,(t)}\right) \times 100 \tag{34}$$

$$PtV = \left(\frac{D(t)^{max} - D(t)^{min}}{D(t)^{max}}\right) \times 100 \tag{35}$$

To assess the participation of the customers at each hour of the introduced demand response programs, we proposed a new measure that is called participation percentage (PP):

$$PP = \left(\frac{L_{curb,j}^{t}}{L_{curb,j}^{max}}\right) \times 100 \tag{36}$$

The following equation can be used to evaluate changes in the utility's profit:

$$Changes\ in\ Profit = \left(\frac{Profit_{Dynamic\ EP} - Profit_{fixed\ EP}}{Profit_{fixed\ EP}}\right) \times 100 \tag{37}$$

In Eqs. 32 to 37, $Load_{Total}^{New}$ is the new total load demand; $Load_{Total}^{Old}$ is the old total load demand; $D_i(t)$ is the load demand of customer i at time t; $D(t)^{min}$ and $D(t)^{max}$ are the maximum and minimum of the load demand; $L_{curb,j}^{max}$ is the maximum curbed load of customer j; $Profit_{Dynamic\ EP}$ is the profit gained by dynamic energy pricing scheme; $Profit_{fixed\ EP}$ is the profit gained by fixed energy pricing scheme.

Chapter 5: Optimization Algorithms

5.1 Fuzzy analytic hierarchical process – non-linear programming (FAHP-NLP)

During the optimization process, the system operator's ability to accurately determine each criterion weighting is critical since it leads to the attaining of the best dispatch plan while maintaining system reliability and resiliency. As the result, to accurately specify the weighting of each criterion of the DCEED problem, we used a fuzzy analytic hierarchy process (AFHP, [59]) approach using a geometric average technique in combination with non-linear programming. The AFHP method can be adapted to the proposed DCEED by following these steps:

Table 5.1: FAHP value structure

Numeric Scale Values	***Fuzzy Values***	***Respective linguistic Terms***
1	$\langle 1,1,1\rangle$	equal importance
3	$\langle 2,3,4\rangle$	moderate importance
5	$\langle 4,5,6\rangle$	strong importance
7	$\langle 6,7,8\rangle$	very strong importance
9	$\langle 9,9,9\rangle$	extreme importance
2,4,6,8	$\langle 1,2,3\rangle,\ldots,\langle 7,8,9\rangle$	intermediate values
1/3, 1/5, 1/7, 1/9	$\langle \frac{1}{4},\frac{1}{3},\frac{1}{2}\rangle,\ldots,\langle \frac{1}{9},\frac{1}{9},\frac{1}{9}\rangle$	values for inverse comparison

- Step 1: Identify the objectives to be achieved.
- Step 2: Identify the criteria that contribute to achieving the objective.
- Step 3: Construct a pairwise comparison matrix among the criteria using a scale of relative importance (as described in Table 5.1) to establish their priority.

$$\hat{A} = \begin{bmatrix} \langle 1,1,1\rangle & \widehat{a_{12}} & \cdots & \widehat{a_{1n}} \\ \widehat{a_{21}} & \langle 1,1,1\rangle & \cdots & \widehat{a_{2n}} \\ \vdots & \vdots & \ddots & \vdots \\ \widehat{a_{n1}} & \widehat{a_{n2}} & \cdots & \langle 1,1,1\rangle \end{bmatrix} \tag{38}$$

$$\hat{a}_{ij} = \langle l_{ij}, m_{ij}, u_{ij}\rangle \tag{39}$$

$$(\hat{a}_{ij})^{-1} = \frac{1}{\hat{a}_{ij}} = \langle \frac{1}{u_{ij}}, \frac{1}{m_{ij}}, \frac{1}{l_{ij}}\rangle \tag{40}$$

In the Eq. 40, the following parameters represent components of fuzzy numbers used to deal with the inherent uncertainty and vagueness in the pairwise comparison process. These parameters are:

$\hat{a}_{ij}$: This typically represents the fuzzy synthetic extent value associated with the pairwise comparison of alternatives i and j. This value aims to encapsulate a holistic measure of preference in the face of uncertainty.

u_{ij}: This stands for the upper bound of the fuzzy number representing the comparison of alternatives i and j. It represents the maximum possible preference value for alternative i over alternative j, capturing the optimistic estimate.

m_{ij}: This represents the mid-value or the most likely value of the fuzzy number associated with the comparison of alternatives i and j. It stands for the most probable preference value for alternative i over alternative j, depicting a realistic or most likely estimate.

l_{ij}: This is the lower bound of the fuzzy number representing the comparison of alternatives i and j. It signifies the minimum possible preference value for alternative i over alternative j, embodying the pessimistic estimate.

λ: is the Lagrangian multiplier.

w_k: is the calculated weights.

The use of these fuzzy numbers, including upper, middle, and lower bounds, enables a more nuanced and flexible evaluation of alternative options in the decision-making process, accommodating the inherent subjectivity and uncertainty in human judgments.

- <u>Step 4</u>: Calculates the Fuzzy weights. In this study, we have used the nonlinear programming (NLP) method to determine the optimal weights:

Max λ

subject to

$$\hat{a}_{ij} - l_{ij} \geq \lambda(m_{ij} - l_{ij}); \hat{a}_{ji} - l_{ji} \geq \lambda(m_{ji} - l_{ji}) \tag{41}$$

$$u_{ij} - \hat{a}_{ij} \geq \lambda(u_{ij} - m_{ij}); u_{ji} - \hat{a}_{ji} \geq \lambda(u_{ji} - m_{ji}) \tag{42}$$

where

$$\hat{a}_{ij} = \frac{w_i}{w_j}; \hat{a}_{ij} = \frac{w_j}{w_i} \ \forall\ i = 1, \ldots, n; j = 2, \ldots, n; j > i \tag{43}$$

$$\sum_{k=1}^{n} w_k = 1; w_k > 0 \tag{44}$$

- Step 5: Calculate the crisp priority vector w from $\hat{A}$ of order n by estimating the solution ratios (a_{ij}) that would maximize λ.
- Step 6: Calculate the global priority weights of these alternatives concerning the defined goal.
- Step 7: The computed weights are defuzzified and expressed in percentages using the center of area (COA) technique.

5.2 Enthusiasm-aided Teaching and Learning Based Optimization coupled with an Enhanced Particle Swarm Optimization (EaTLBO-EPSO)

To enhance the efficiency of enthusiasm-aided teaching and learning-based optimization (EaTLBO) and the enhanced particle swarm optimization (EPSO), a sequential architecture was employed to synergistically integrate these two algorithms. Subsequently, each algorithm's foundational principles and mathematical underpinnings will be explicated comprehensively. Once the fundamental concepts are elucidated, a visual representation in the form of a flowchart will be employed to facilitate a deeper comprehension of the combination process that underlies this hybrid approach.

5.2.1 Enthusiasm Aided Teaching and Learning Based Optimization (EaTLBO)

Rao et al. [60] introduced the teaching-learning-based optimization (TLBO) algorithm less than a decade ago, based on the principles of teaching and learning in a classroom. TLBO's core concept is inspired by the impact of a teacher on the learning outcome of learners and the interaction between learners. The outputs interpret in terms of grades and express the teachers' and learners' teaching and learning ability. Similar to the other evolutionary algorithms and swarm intelligence methods such as genetic algorithms (GAs), differential evolution (DE), particle swarm optimization (PSO), cultural algorithm (CA), etc., TLBO is a population-based optimization method. However, unlike the others, it has no adjusting parameters besides its population size and the maximum number of iterations. The TLBO process can be divided into two phases: (i) the teaching phase and (ii) the learning phase. The teaching phase emulates the learning procedure from a teacher, while the learning phase imitates the learning process through interaction between learners in a class [61]. To enhance the basic TLBO's performance in this study, an enthusiasm learning mechanism was implemented for both algorithm phases. The proposed algorithm, called EaTLBO, is described in detail in the following subsections.

5.2.2 Teaching Phase according to Enthusiasm Learning Mechanism

In the basic TLBO, the teaching and learning phases provide the same opportunity for the learners to acquire knowledge from the teacher and classroom interactions. However, in reality, the learners' enthusiasm differs from each other in a classroom. Generally, learners with higher enthusiasm would be able to obtain more knowledge from others. In contrast, the less focused and motivated learners have a lower possibility of learning. To incorporate the enthusiasm learning mechanism (ELM) into TLBO's basic teaching strategy, the following assumption must be considered: learners who have achieved good grades are more likely to acquire knowledge from the teacher than those with lower grades.

The proposed algorithm begins by sorting the learners based on their fitness values, from best to worst.

$$f(x_1) \le f(x_2) \le \cdots \le f(x_{N_{pop}}) \tag{45}$$

Next, the learning enthusiasm (LE) values will be calculated for each learner:

$$LE_i^T = FVBL_{int} + (FVBL_{int} - FVWL_{int})\frac{TN_{pop} - Pop}{TN_{pop}} \tag{46}$$

$FVBL_{int}$ = The fitness value of the best learner following the initialization stage

$FVWL_{int}$ = The fitness value of the worst learner following the initialization stage

TN_{pop} = Total number of populations

$Pop = 1,2,3 \ldots N_{pop}$

After determining the LE values, learners with higher LE values will be motivated to learn from the teacher. A random number (R_i) between 0 and 1 will be generated for each learner. If R_i is less than or equal to the learner's LE value (LE_i^T), the learner will learn from the teacher. Otherwise, it will disregard the teacher's knowledge. The learner x_i will update its position using the following equation.

$$x_i^{new} = \begin{cases} V_i & if \quad R_i \le 0.5 \\ U_i & otherwise \end{cases} \tag{47}$$

$$V_i = x_i^{old} + rand_1(Varsize) \times (x_{teacher} - TF \times Mean) + rand_2(Varsize) \times \left(x_{teacher} - x_i^{old}\right) \tag{48}$$

$$U_i = abs\big((0.9 - \Theta)\, x_r^1 + \Theta \times (x_r^2 - x_r^3)\big) \tag{49}$$

where $rand_1(Varsize)$ and $rand_2(Varsize)$ are randomly generated numbers between 0 and 1, with their sizes based on the number of variables; TF is the teaching factor and it is equal to $round[1 + rand(0,1)]$; $x_{teacher}$ is the value of the best learner which has been selected as a teacher; $Mean$ is the mean value of all the learners in the population; x_r^1, x_r^2 and x_r^3 are integers randomly generated according to $Varsize$ ($x_r^1 \ne x_r^2 \ne x_r^3 \ne iteration\ number$); Θ is the multiplicative factor (it varies from 0.1 to 0.5) and x_i^{old} is the original or the initialized value of the learners. If the updated position of the learner (x_i^{new}) is an improvement over its previous position, the updated position will replace the previous one. The Eq. 49 diversifies the new population by employing the LE mechanism and improves the search directions in each iteration.

5.2.3 Learning Phase according to Enthusiasm Learning Mechanism

A learning enthusiasm-based strategy, similar to the ELM for the teaching phase, has been introduced to improve the learning phase's efficiency. Learners are ranked based on their fitness values obtained in the teaching phase, and a new LE evaluation process is conducted for the learning phase.

$$LE_i^{Learn} = FVBL_{Learn} + (FVBL_{Learn} - FVWL_{Learn})\frac{TN_{pop} - Pop}{TN_{pop}} \tag{50}$$

$FVBL_{Learn}$ = fitness value of the best learner after the teaching phase

$FVWL_{Learn}$ = fitness value of the worst learner after the teaching phase

During the learning phase, learners are ranked based on their fitness values obtained during the teaching phase, and their learning enthusiasm (LE) values are then calculated. A random number R_i (that is between 0 and 1) is generated for each learner, and if $R_i \leq LE_i^{Learn}$, the learner will learn from others. If the criteria are met, the learner (x_i) will update its position:

$$x_i^{new} = \begin{cases} x_i^{old} + rand(Varsize) \times (x_i - x_j) & if \quad f(x_i) \leq f(x_j) \\ x_i^{old} + rand(Varsize) \times (x_j - x_i) & if \quad f(x_i) > f(x_j) \end{cases} \tag{51}$$

The selected learners x_i and x_j have fitness values $f(x_i)$ and $f(x_j)$, respectively. If the new position of learner (x_i^{new}) is better than its old position, it will replace the old position, while considering the fitness values of x_i and x_j.

5.3 An Enhanced Particle Swarm Optimization (EPSO)

For the first time in 1995, the particle swarm optimization (PSO) algorithm was introduced by J. Kennedy and R. Eberhart [62]. The PSO has been structured based on the social and natural behavior of animal groups such as schools of fish and flocks of birds. A population of individuals, which are particles, adapts their movements toward the food sources that have been successfully traced before [63]. PSO has two primary operators; velocity (which determines the directions of the particles) and position (which defines the location of the particles in the search space). In each generation, the velocity of the particles will be determined by means of its current velocity, distance from the best position of each particle (local best position), and distance from the best position of the entire population (global best position). In the subsequent stage, the locations of the particles can be assessed with respect to the previous positions and the new velocities of the particles. This process will be iterated a number of times or until it reaches the stopping criteria [64].

The location of each particle within the search space is ascertained through a careful evaluation of its preceding position and the corresponding particle velocity. This methodology ensures a dynamic and evolving exploration of the solution space, thereby refining the process of optimizing the objective function. Thus, the mathematical formulation of PSO can be described by updating the position of each particle:

$$\vec{x}_i(t+1) = \vec{x}_i(t) + \vec{V}_i(t+1) \tag{52}$$

The velocity is updated based on the particle's current velocity, the distance to its personal best position ($\vec{P}_i(t)$), and the distance to the swarm's global best position ($g(t)$). Therefore, the equation for updating the vector of velocity can be formulated as:

$$\vec{V}_i(t+1) = \vec{V}_i(t) + C_1(\vec{P}_i(t) - \vec{x}_i(t)) + C_2\big(g(t) - \vec{x}_i(t)\big) \tag{53}$$

In Eqs. 52 and 53, $\vec{x}_i(t)$ is the position of particle at the time t; $\vec{V}_i(t)$ is the velocity of the particle at the time t; $\vec{V}_i(t+1)$ is the updated velocity of the particle at the time t.

Equations Eq. 52 and 53 are representing the basic version of PSO; however, several modifications are essential to be made in order to improve its performance. The proposed improvements are stated as below:

<u>5.3.1 Cognitive improvement:</u> improving the performance of random cognitive and social coefficients based on the uniformly distributed random numbers between 0 and 1, where the size of variables defines the length of these numbers.

$$\begin{aligned}\vec{V}_{ij}(t+1) = \vec{V}_{ij}(t) + &\overbrace{(1 - r_1(Var_{size}))C_1(\vec{P}_{ij}(t) - \vec{x}_{ij}(t))}^{Cognitive\ Component(I)} \\ &+ \overbrace{(1 - r_2(Var_{size}))C_2(g_j(t) - \vec{x}_{ij}(t))}^{Social\ Component(II)}\end{aligned} \tag{54}$$

In Eq. 54, $\vec{V}_{ij}(t)$ is the vector of velocity concerning j^{th} component; $\vec{V}_{ij}(t+1)$ is the updated vector of velocity concerning j^{th} component; $\vec{P}_{ij}(t)$ is the best position that the i^{th} particle has achieved at time t in the j^{th} dimension; $\vec{x}_{ij}(t)$ is the position of the i^{th} particle in the j^{th} dimension at time t; C_1 and C_2 are random number in the range of [0, 1]; Var_{size} is the variable size.

5.3.2 Constriction coefficients technique: to assist the vector of velocity in selecting precise directions in the search space, this study has used the constriction coefficient technique (CCT).

$$\chi = \frac{2\mathrm{K}}{\left|2 - \varphi + \sqrt{\varphi^2 - 4\varphi}\right|} \tag{55}$$

$$\varphi = \varphi_1 + \varphi_2 \geq 4.1, \ \ and \ 0 \leq \mathrm{K} \leq 1 \tag{56}$$

$$C_1^{CCT} = \chi\varphi_1 \quad and \quad C_2^{CCT} = \chi\varphi_2 \tag{57}$$

In this regard, in the Eq. 54 C_1 and C_2 will be substituted by C_1^{CCT} and C_2^{CCT}.

In Eqs. 55, 56 and 57, χ is the constriction coefficient; φ is the sum of the acceleration coefficients (φ_1 and φ_2); C_1^{CCT} and C_2^{CCT} are the new cognitive and social acceleration coefficients, respectively.

5.3.3 Time-varying damping inertia weight (TVDIW): to create a suitable trade-off between the exploration and exploitation during the optimization process, this study has proposed an innovative non-linear time-varying formulation for the inertia weight of PSO. The inertia weight specifies the contribution rate of the previous velocity of each particle in evaluating the new velocity at the current iteration.

$$W_{Damp} = \ W_{Damp}^{Max} \times \left[\left(W_{Damp}^{Max} - W_{Damp}^{Min} - \alpha_1\right) \exp\left(\frac{1}{1 + \ \alpha_2 \times \frac{Iter_i}{Max_{Iter}}}\right)\right] \tag{58}$$

The previous formulation for the vector of velocity can be rewritten as:

$$\begin{aligned} \vec{V}_{ij}(t+1) = \ & \overbrace{W_{Damp}\vec{V}_{ij}(t)}^{Inertia\ Component\ (I)} + \overbrace{(1 - r_1(Var_{size}))\ C_1^{CCT}\ (\vec{P}_{ij}(t) - \vec{x}_{ij}(t))}^{Cognitive\ Component(II)} \\ & + \overbrace{(1 - r_2(Var_{size}))\ C_2^{CCT}\ (g_j(t) - \vec{x}_{ij}(t))}^{Social\ Component(III)} \end{aligned} \tag{59}$$

where W_{Damp}^{Max} and W_{Damp}^{Min} are the maximum and minimum damping ratio and their assigned values are 0.9 and 0.4, respectively; α_1 and α_2 are the damping inertia coefficients and their values are 0.2 and 7, respectively; $Iter_i$ is the current iteration and Max_{Iter} is the maximum number of iterations.

5.3.4 Particle clipping constraint: to ensure that the movement particles are within the boundaries of the objective function, this study has proposed a formulation to maintain and rectify the position of the particles.

$$x_i(t+1) = \begin{cases} x_i^{Max} & if \quad x_i(t+1) > x_i^{Max} \\ x_i(t+1) & if \quad x_i^{Min} \leq x_i(t+1) \leq x_i^{Max} \\ x_i^{Min} & if \quad x_i(t+1) < x_i^{Min} \end{cases} \tag{60}$$

In Eq. 60, x_i^{Min} and x_i^{Max} are the upper and lower bound of the particles positions in PSO algorithm.

5.3.5 A modified crossover operator: to guarantee that at each iteration an appropriate diversification process will be conducted on the entire particles, this study has presented a robust crossover operator. Another functionality of this operator is to avoid the re-exploration of undesirable regions that have been searched previously.

$$x_i(t+1) = \begin{cases} x_i(t+1) \quad if \quad rand_i(Pop_{number}, Var_{size}) \leq CO_{ratio} \\ P_i(t) \quad\quad Otherwisse \end{cases} \tag{61}$$

In Eq. 61, $x_i(t+1)$ is the updated position of the particle; $rand_i(Pop_{number}, Var_{size})$ is the random number generator based on the population number (Pop_{number}) and the variable size (Var_{size}); CO_{ratio} is the ratio of the crossover operator.

Chapter 6: Results and Discussions

In this chapter, we have applied the proposed methods to a realistic simulation environment using a variety of factors to evaluate their performance in practice. This section contains two case studies that look at various viewpoints and technical problems that energy markets faces across the world.

The first case study aims to evaluate the performance of the proposed FAHP-NLP method in comparison to the FAHP and weighted-sum-average (WSA) methods in defining multi-criteria weights, and to demonstrate the effectiveness of the EaTLBO-EPSO algorithm in solving the multi-criteria security-constrained DCEED problem. In the second case study, the profit-based scheduling formulation is used to test the maximization of profit in a deregulated power market environment, with a focus on customer-centric demand management plans to mimic DR program interactions.

The mentioned case studies were chosen primarily to illustrate that the CC-GTDR and DCEED can be done simultaneously on the supply and demand sides, rather than examining them separately without reciprocal impacts. As a result, the test systems investigated in this study have two sides: a utility side and a consumer side. The utility provides generating supply for the aggregated residential customers with different pricing options such as fixed energy pricing, ToU prices, and RTP rates. Additionally, the CC-GTDR allows customers to respond to market pricing by specifying their desired ToU rates through a participation factor.

To have a clearer picture of the designed CC-GTDRP and deregulated market environment, the following assumptions were considered:

1) The value of power interruptibility (λ) specifies the cost of not providing electricity to a given place in the power grid or to a connected customer, and it is defined by locational marginal pricing (LMPs).
2) Customers must notify the utility in advance about their daily interruptible power limit and hourly outage cost factors. Similarly, energy prices (EPs) should be announced to customers within organized timeframes by the utility.
3) To prevent jeopardizing customers’ regular operations, the utility cannot curtail more than 12% of a customer’s daily allotment of interruptible power during each hour of DR program operation.
4) Customers will be compensated based on their level of curtailed electricity per the hour. Higher incentives will be given to customers who have more curtailed power.

6.1 First Case Study

6.1.1 Preliminary Technical Details – Case Study 1

This research has devised a hybrid optimization method (EaTLBO-EPSO) to address the stated multi-criteria security-constrained DCEED problem. The ETLBO-EPSO is compared to the combined genetic algorithm and particle swarm optimization (GA-PSO), the grey wolf optimization algorithm (GWOA), the artificial bee colony optimization (ABCO), and the harmonic search optimization (HSO) to reveal its effectiveness. The applied FAHP-NLP method determines the DCEED criteria weights. The ten thermal generating units test system is used to verify the described techniques. References [65, 66] provides extensive operational information on the examined test system, where the load curve hourly values are tabulated in Table 6.1. To correctly study the performance of the constrained techniques, the EaTLBO-EPSO was carried out for 24 hours. The system's total daily permitted emission volume is 67000 lb. The weights of the criteria, namely $W^{Gen}, W^{EM}, W^{resv}$ and W^{SCEI}, were calculated to be 60%, 15%, 20%, and 5%, respectively, using the proposed FAHP-NLP approach. It is worth noting that the determination of these weights was based on the relevance of each criterion in the optimization process. The FAHP-NLP method established the interrelationships among the criteria, prioritizing the generation of higher profits for the system operator while respecting the interests of the consumers.

Table 6.1: Ten units' test system hourly load curve

Time (h)	***Operation Status***	***Load Demand (MW)***
1	***Off-Peak***	***945***
2	***Off-Peak***	***930***
3	***Off-Peak***	***920***
4	***Off-Peak***	***1100***
5	***Off-Peak***	***1200***
6	***Off-Peak***	***1300***
7	***Partial-Peak***	***1400***
8	***Partial-Peak***	***1480***
9	***Peak***	***1650***
10	***Peak***	***1700***
11	***Peak***	***1780***
12	***Peak***	***1800***
13	***Peak***	***1845***
14	***Peak***	***1730***
15	***Partial-Peak***	***1550***
16	***Partial-Peak***	***1460***
17	***Partial-Peak***	***1420***
18	***Peak***	***1500***
19	***Peak***	***1580***
20	***Peak***	***1620***
21	***Peak***	***1650***
22	***Off-Peak***	***1350***
23	***Off-Peak***	***1160***
24	***Off-Peak***	***1070***

6.1.2 Explanation of Results – Case Study 1

To provide holistically and a detailed evaluation, the obtained results of the proposed method (FAHP-NLP) is compared with another 2 methods (FAHP and WSA) that have been developed recently in the same field of study [65]. Table 6.2 show that EaTLBO-EPSO outperformed the other optimization methods by achieving considerably lower values in all criteria. FAHP-NLP has improved the performance of EaTLBO-EPSO by determining optimal criterion weights, leading to superior results compared to other methods. As a result, we will employ a combination of EaTLBO-EPSO and FAHP-NLP to solve the multi-criteria security-constrained DCEED problem in the subsequent case study. Also, Fig. 6.1 provides a visual illustration of generators' schedules that have been obtained by the combination of FAHP-NLP and EaTLBO-EPSO for the analyzed operation day.

Table 6.2: Evaluation of various optimization and weighting approaches

FAHP-NLP Weighting Method					
Compared Algorithms	***EaTLBO-EPSO***	***GA-PSO***	***GWOA***	***ABCO***	***HSO***
Cost of Generation ($)	1888185.47	1893158.18	1898283.25	1901001.92	1903389.05
Emission Cost ($)	32225.23	32362.11	32325.54	32164.24	32468.75
Reserve Cost ($)	98093.45	98148.76	98130.07	98109.17	98158.34
Socio-economic Cost ($)	14889.18	14925.39	14915.71	14906.09	14908.92
FAHP Weighting Method					
Compared Algorithms	***EaTLBO-EPSO***	***GA-PSO***	***GWOA***	***ABCO***	***HSO***
Cost of Generation ($)	1888209.28	1893179.29	1898304.76	1901015.07	1903403.68
Emission Cost ($)	32280.65	32700.91	32371.54	32348.96	32703.43
Reserve Cost ($)	98095.75	98205.18	98131.24	98182.55	98159.93
Socio-economic Cost ($)	14922.27	14956.41	14946.30	14937.20	14939.76
WSA Weighting Method					
Compared Algorithms	***EaTLBO-EPSO***	***GA-PSO***	***GWOA***	***ABCO***	***HSO***
Cost of Generation ($)	1906292.51	1909519.47	1913727.59	1917145.47	1924387.32
Emission Cost ($)	32745.38	32363.19	32336.10	32168.40	32481.83
Reserve Cost ($)	98140.10	98154.60	98169.28	98111.38	98179.68
Socio-economic Cost ($)	14972.63	14966.83	14955.13	14946.79	15015.01

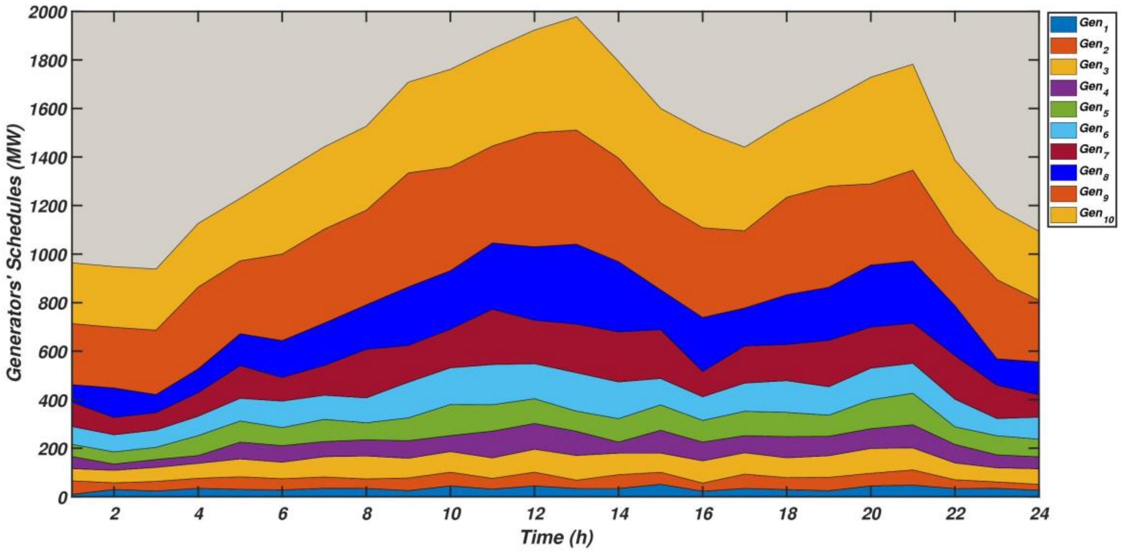

Figure 6.1: Generators' schedules for first case study

6.2 Second Case Study

6.2.1 Preliminary Technical Details – Case Study 2

The test system for this case study includes ten thermal generating units and seven aggregated residential customers with a daily load profile of 34140 MW. The utility budget for implementing the CC-GTDR is \$100,000 per day, and the hourly values of power interruptibility are based on the PJM electricity market and regional transmission operator (RTO) and presented in Table 6.3. The remainder of the customers' associated information can be found in [65]. In this case study, we have used three different energy prices: fixed prices, ToU prices, and RTP prices, which are shown in Fig. 6.2 along with the maximum expected hourly load curtailment that the customers would be able to achieve.

In this test system, four of the ten generators (Gen_1, Gen_3, Gen_9 and Gen_{10}) have multiple prohibited operating zones (POZs) that add complexity to the optimization process. The EaTLBO-EPSO algorithm is proposed to find the optimal solution while considering the system's physical, operational, and systematic constraints, including the NOx emission reduction constraint. The calculated criteria weights ($W^{Gen}, W^{EM}, W^{resv}, W^{CSEI}, W^{RES}$ and W^{GTDR}) for this case are 48%, 10%, 12%, 3%, 7% and 20%, respectively.

Table 6.3: Hourly measurements of power interruptibility

λ	C_1	C_2	C_3	C_4	C_5	C_6	C_7
1	31.21	30.17	30.18	30.05	29.78	29.76	28.62
2	29.14	27.84	27.72	27.97	27.33	27.45	26.55
3	26.94	26.68	26.03	25.9	25.88	25.77	25.26
4	27.2	26.17	26.12	26.31	25.81	25.77	24.87
5	28.1	27.2	27.07	26.68	26.55	26.57	26.03
6	33.93	33.28	32.76	32.89	32.37	32.25	31.6
7	38.02	35.87	35.74	35.87	35.35	35.22	34.32
8	37.81	36.01	36.13	36.14	35.61	35.74	34.32
9	39.24	37.55	37.94	37.43	37.17	37.04	35.48
10	45.45	43.63	43.25	42.86	42.47	42.34	40.4
11	48.04	46.35	46.1	45.58	45.45	45.32	43.12
12	40.4	38.85	38.59	38.46	38.33	38.2	36.65
13	41.57	39.24	39.5	39.24	38.97	38.84	37.04
14	42.6	41.05	40.27	40.31	39.75	39.79	38.46
15	39.5	37.68	37.42	37.39	37.16	37.04	35.1
16	42.86	41.05	40.79	40.92	40.66	40.53	38.72
17	43.12	41.31	41.95	41.82	41.57	41.7	39.11
18	46.61	44.29	44.41	44.16	43.77	43.51	41.57
19	41.57	39.49	40.14	39.62	39.88	40.01	37.68
20	41.57	39.11	40.4	39.75	39.76	39.88	37.3
21	119.87	113.92	114.31	113.79	113.4	113.27	107.7
22	44.29	42.34	42.55	41.82	41.56	41.44	39.88
23	32.89	31.73	32.21	30.95	31.08	30.95	30.18
24	32.9	31.75	32.19	30.91	30.97	30.85	30.11

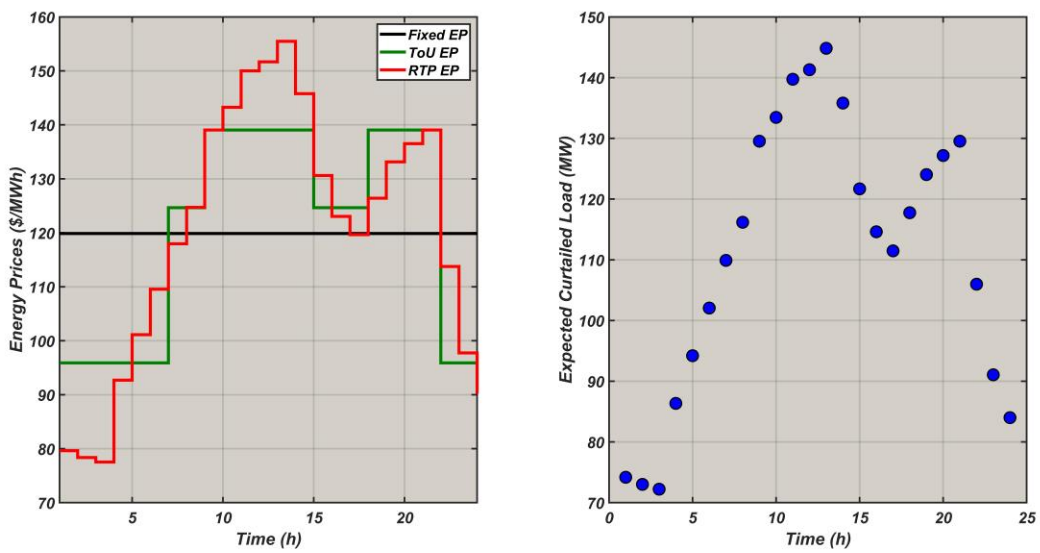

Figure 6.2: Different energy prices and maximum expected hourly load curtailments

6.2.2 Investigated Scenarios – Case Study 2

This case study examines 3 base cases and 5 realistic scenarios that can occur in a liberalized electricity market. Their goals and details are fully described in the following:

- Basic Case - Fixed EP: In the absence of GTDR implementation, the maximization of utility profit and social welfare are obtained through fixed energy prices.
- Basic Case - ToU EP: The utility profit and social welfare are maximized using ToU energy prices without implementing GTDR.
- Basic Case - RTP EP: The profit and social welfare maximization is performed similar to the previous case (ToU EP) but using RTP energy prices instead.
- Scenario 1: This case aims to maximize the utility profit and social welfare through the implementation of GTDR while using fixed energy prices.
- Scenario 2: In Scenario 2, the utility profit and social welfare are maximized through ToU energy prices with the implementation of GTDR.
- Scenario 3: The utility profit and social welfare are maximized through RTP energy prices with the implementation of GTDR.
- Scenario 4: CC-GTDR is used to maximize utility profit and social welfare through the implementation of RTP-EP and ToU customers' announced costs.
    - The sum of customers' outage cost coefficients as well as their respective ToU participation factors is shown in Fig. 6.3.
- Scenario 5: In this scenario, the goal is to maximize the utility's profit and social welfare while also incorporating the power output of renewable energy resources (RESs) and the customer-centric GTDR program into the system. This is achieved by optimizing the use of RTP-EP pricing and taking into account the announced costs of ToU customers.
    - The RESs are consisting of two sources: wind and solar energies. The system under study includes a wind farm and a PV power plant with a total capacity of 614 MW, which is more than 33% of the system peak load. The wind farm consists of 138 Enercon E-115 WTGs, generating a total output of 414 MW, while the PV power plant comprises 909,091 SolatGate-2200 PV modules, with an aggregated capacity of 200 MW. Figs. 6.4 and 6.5 illustrate the power output and forecasted power of the RESs, respectively.

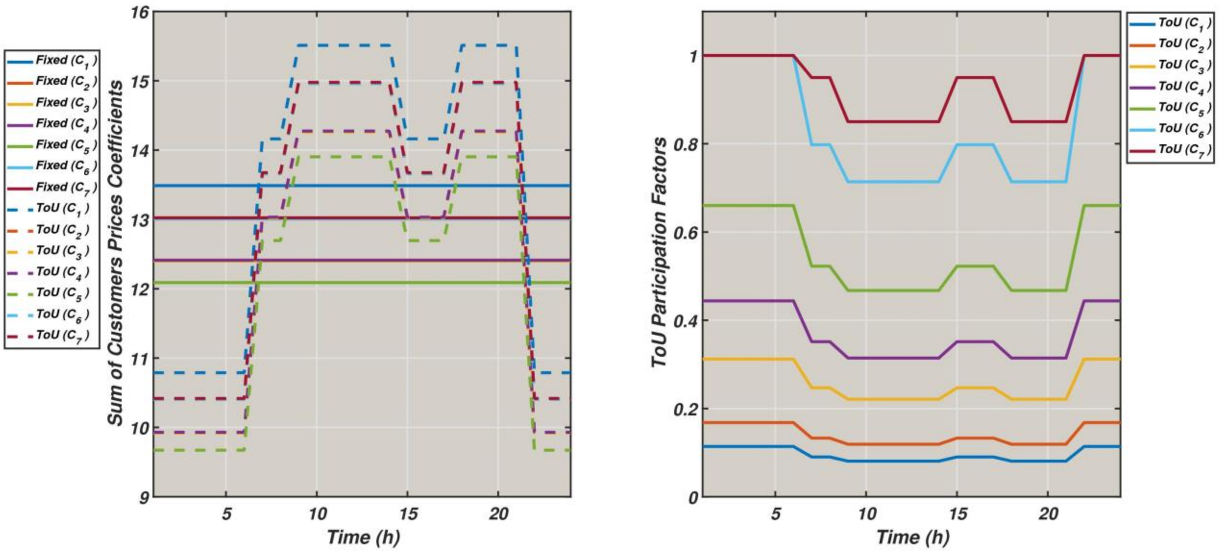

Figure 6.3: Sum of customers' outage cost coefficients and their respective ToU participation factors

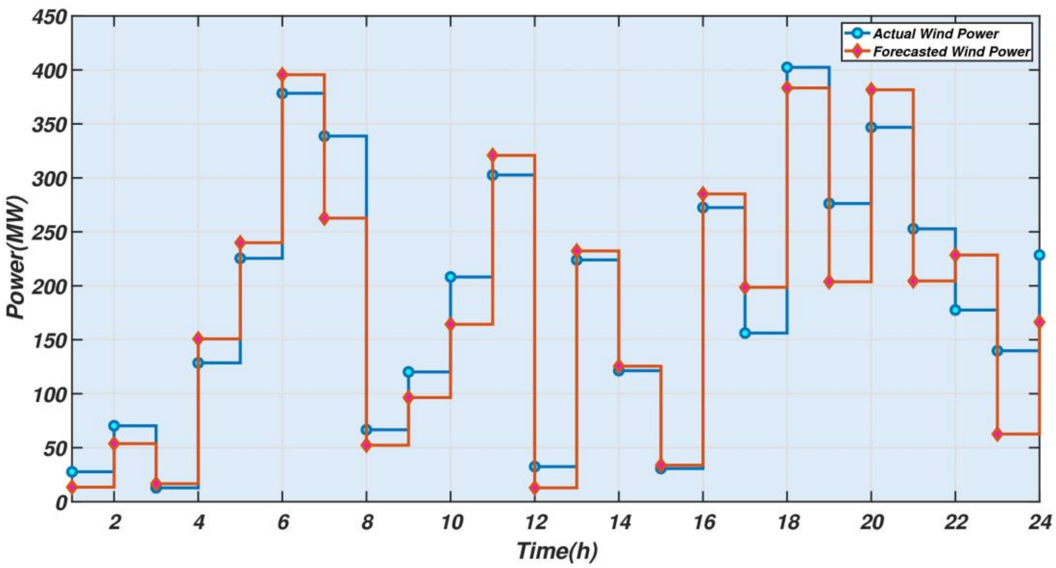

Figure 6.4: The forecasted and actual power output of the connected wind farms

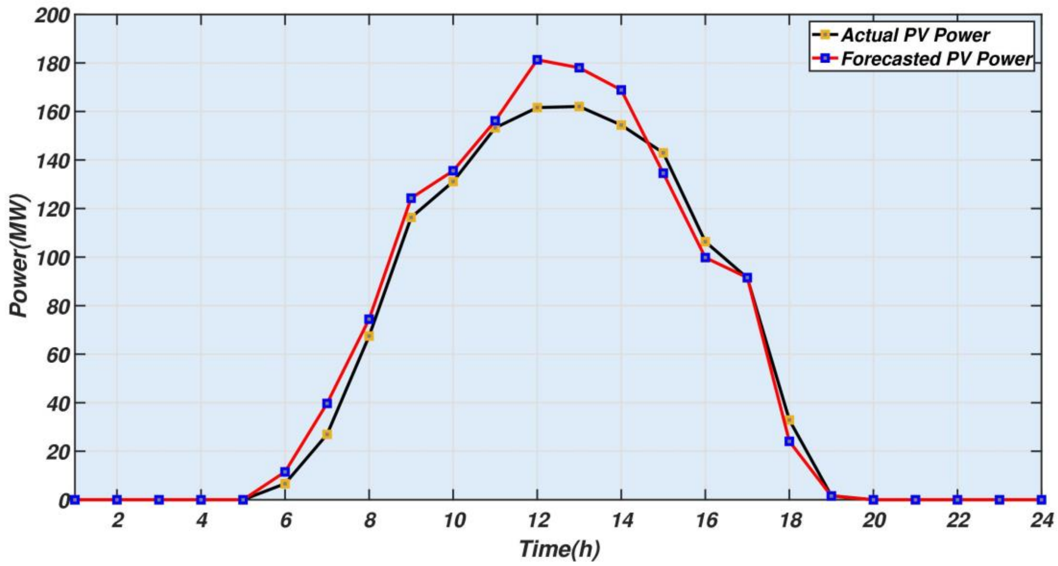

Figure 6.5: The forecasted and actual power output of the connected PV power plants

6.2.3 Explanation of Results – Case Study 2

Fig. 6.6 shows the reduced load curves of different scenarios after the implementation of CC-GTDR and their corresponding participation percentages (PP). From Fig. 6.6 it is evident that Scenario 4 has achieved the highest level of participation during the partial-peak and peak hours, where its highest PP is 98.48% at the 13:00 pm. Nevertheless, on the contrary it has shown the lowest interest in the load curtailment during the off-peak hours as the incentives are not profitable enough based on the intelligent assessment of Scenario 4's formulation. Furthermore, it is significant to mention that the Scenario 4 has maintained its PP above 80% throughout the partial-peak and peak hours which reveals the successful implementation of CC-GTDR along with real-time energy prices (RTP-EP). The second-best scenario appeared to be the Scenario 3 that is being followed by Scenarios 2, 1 and 5, respectively. The hourly curtailed power and incentives received by each customer for Scenarios 1, 2, and 3 are illustrated in Fig. 6.7.

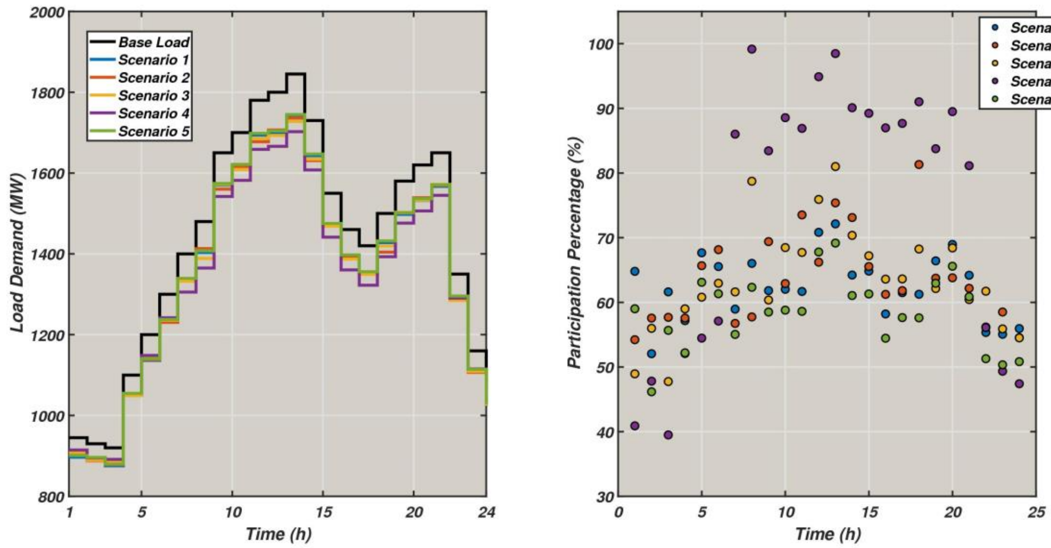

Figure 6.6: The hourly load curves after CC-GTDR implementation and their respective participation percentages (Scenarios 1 to 5)

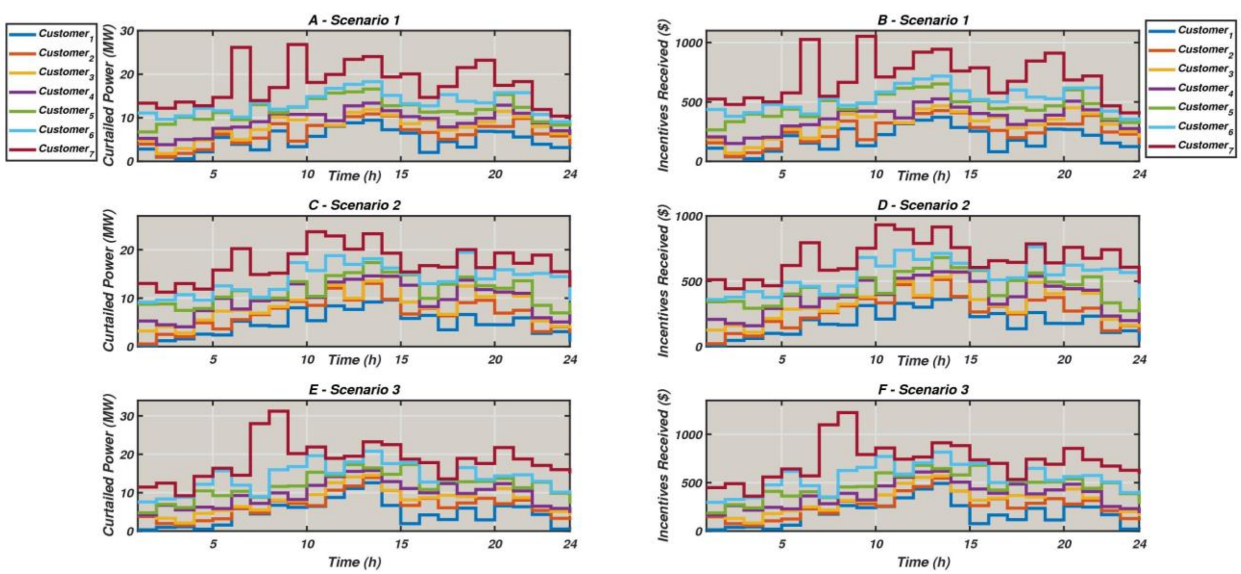

Figure 6.7: Hourly load curtailment and their corresponding incentive payments (Scenarios 1 to 3)

In Scenario 4, the pricing mechanism has encouraged customers to reduce their power consumption during peak hours, which has resulted in a flatter load profile, as seen in Fig. 6.8. This is an important aspect of CC-GTDR, as it helps the system operator to balance the load and avoid any potential blackouts or brownouts.

6.2.4 Inclusion of Renewable Energy Resources (RESs)

In Scenario 5, the inclusion of RESs has had an impact on the load curtailment process due to their intermittent nature. This is because the power output from RESs can vary depending on weather conditions such as wind and sunlight, which can lead to fluctuations in the load curtailment process. However, the inclusion of RESs in the energy mix is a crucial step towards a more sustainable and eco-friendly energy system. By replacing some of the thermal generators (in this case G_1 and G_3) with RESs, the system operator can reduce emissions and diversify the energy mix, which can lead to a more stable and resilient power system. Overall, as depicted in Fig. 6.8, the results from Scenarios 4 and 5 highlight the importance of carefully balancing the supply and demand sides of the energy system, considering the impact of various factors such as pricing mechanisms, RESs, and load curtailment strategies.

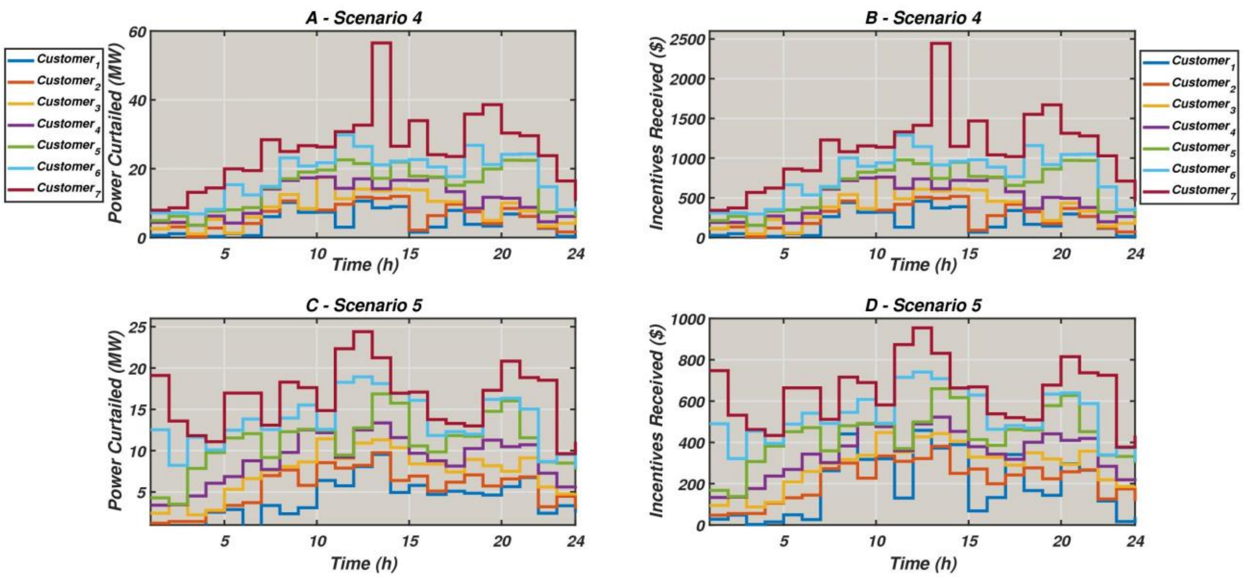

Figure 6.8: Hourly load curtailment and their corresponding incentive payments (Scenarios 4 and 5)

Table 6.4 presents the load analysis results for all the studied scenarios, where four load indexes are considered: TLR (total load reduction), PLR (peak load reduction), PAR (peak to average ratio), and PtV (peak to valley ratio). The results indicate that the use of RTP pricing in the first three scenarios (1, 2, and 3) has led to improved load performance for all the load indexes. Based on these findings, RTP-EP has been selected as the basis for Scenario 4, which incorporates both ToU customer cost pricing and ToU participation factors to further enhance the rights of customers in the GTDRP implementation.

The results in Table 6.4 show that Scenario 4 has achieved the best performance for all the load indexes. Specifically, the TLR, PLR, PAR, and PtV values for Scenario 4 are 6.11%, 7.73%, 1.2746, and 47.64%, respectively. These results demonstrate the effectiveness of the proposed RTP-EP with ToU customer cost pricing and ToU participation factors in achieving optimal load performance while respecting customer rights in the CC-GTDR implementation.

Table 2.4: Load Analysis after the application of GTDR method

Load Analysis	*Scenario 1*	*Scenario 2*	*Scenario 3*	*Scenario 4*	*Scenario 5*
Total Load Reduction (%)	4.94	5.06	5.09	6.11	4.64
Peak Load Reduction (%)	5.66	5.92	6.36	7.73	5.43
Peak-to-Average Ratio	1.2872	1.2853	1.2797	1.2746	1.2863
Peak-to-Valley (%)	49.70	49.40	48.75	47.64	49.58

Table 6.5 provides an analysis of the utility profit and customer costs for each scenario. The results show that Scenario 4 has the highest load curtailment at 2085.01 MW, followed by Scenarios 3, 2, 1, and 5 with curtailments of 1738 MW, 1727.03 MW, 1688.14 MW, and 1585.12 MW, respectively. In terms of incentives received by customers, the order is the same as the load curtailment, with Scenario 4 offering the highest incentives and Scenario 5 offering the lowest.

In contrast, Scenario 5 provides the highest utility profit at 8.55%, due to the lower production costs of the integrated RES units compared to the thermal generators. It's important to note that in all scenarios, the more load being served by the system operator, the higher the profit obtained. This is because the utility is able to charge higher prices during peak hours when demand is higher, resulting in a higher profit margin.

Table 6.5: Evaluation of utility profit and customers' payment when the CC-GTDR is performed

Studied Scenarios	*Profit ($)*	*Changes in Profit (%)*	*Curtailed Power (MW)*	*Paid Incentives ($)*
Fixed EP	2185245.86	0.00	0.00	0.00
ToU EP	2312451.70	5.82	0.00	0.00
RTP EP	2356866.77	7.85	0.00	0.00
Scenario 1	1887664.67	0.00	1688.14	66262.04
Scenario 2	1994863.71	5.68	1727.03	67793.35
Scenario 3	2031413.52	7.62	1738.00	68225.17
Scenario 4	1980764.58	4.93	2085.01	90181.27
Scenario 5	2049016.40	8.55	1585.12	62011.55

In this study, the spinning reserve requirement (SRR) is satisfied by the generators with no POZ restrictions. In the presence of RESs, the paper has proposed two formulations for precise determination of the regulating and contingency reserves. The total required SRR prior to RESs incorporation is 1991.5 MW, while after their integration is 2126.43 MW. In Fig. 6.9, the impact of the proposed formulations on SRR estimation is presented and compared to traditional methods.

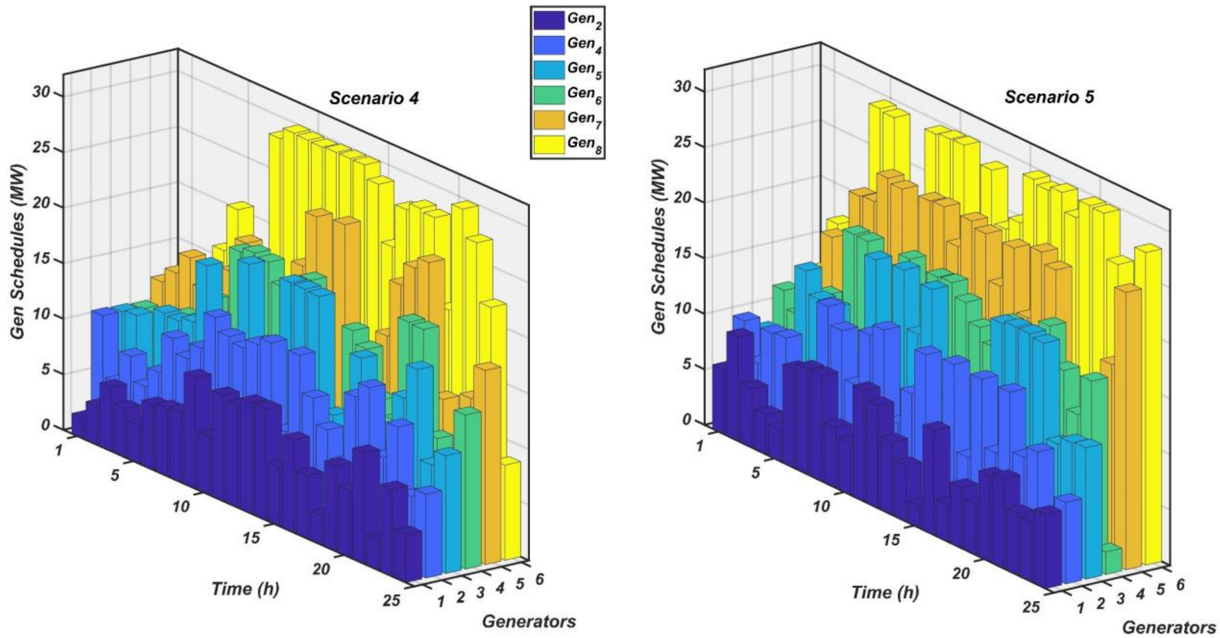

Figure 6.9: Comparison of SRR determination before (Scenario 4) and after (Scenario 5) the integration of RESs

6.2.5 Evaluation of Operating Costs from the Utility Perspective

In addition to the previous results, Tables 6.6 and 6.7 provide a comprehensive cost analysis and operational performance comparison between all the investigated scenarios. The findings show that Scenario 4 outperforms all other scenarios, except for Scenario 5, due to the incorporation of renewable energy sources which significantly impact fuel generation and emission cost savings. Furthermore, all the scenarios have very low PVC violations, with Scenario 4 having the highest frequency of PVC violations due to its complex pricing mechanism. Overall, the results demonstrate the effectiveness and feasibility of the proposed CC-GTDR with the integration of renewable energy sources in enhancing system efficiency and customer welfare while maintaining grid stability and reliability.

Table 6.6: Evaluation of expenses from the utility perspective

Studied Scenarios	*Cost of Generation ($)*	*Cost of Emission ($)*	*Cost of Reserve ($)*	*Cost of socio-economic impact ($)*	*Cost of RESs ($)*	*Total Cost of Generation ($)*
Fixed EP	1892356.43	32286.19	98177.27	15150.73	0.00	2037970.62
ToU EP	1892221.26	32277.05	98158.55	15125.46	0.00	2037782.32
RTP EP	1891568.71	32060.39	98143.04	14998.11	0.00	2036770.25
Scenario 1	1797833.25	27827.47	98108.72	14213.92	0.00	1937983.36
Scenario 2	1795680.23	27794.15	98106.14	14196.89	0.00	1935777.41
Scenario 3	1795070.86	27784.72	98097.78	14192.08	0.00	1935145.44
Scenario 4	1775847.01	26387.68	98097.08	14040.09	0.00	1914371.86
Scenario 5	1455208.5	24725.52	104814.05	14259.14	171600.74	1770607.95

Table 6.7: Assessing the performance of generating units during operational hours

Studied Scenarios	***Released Volume of Emission (lb)***	***PVC Violation Frequency***	***Accumulated PVC***
Fixed EP	65890.22	1.00	1.01E-10
ToU EP	65871.54	1.00	3.87E-9
RTP EP	65429.36	1.00	3.34E-9
Scenario 1	56790.76	2.00	6.35E-11
Scenario 2	56722.65	3.00	5.96E-11
Scenario 3	56703.49	3.00	4.18E-11
Scenario 4	53852.40	6.00	3.22E-15
Scenario 5	50460.25	4.00	6.26E-9

Chapter 7: Conclusions and Future Works

7.1 Conclusions

This study introduces multi-criteria DCEED method coupled with a CC-GTDR formulation, where the designed method calculates the optimal dispatching, customer load reduction, and utility offered incentives while considering several physicals, operational and environmental constraints of generation units. To maintain the stated constraints, a comprehensive power violation constraint handling technique through the utilization of a self-adaptive algorithm implemented. To solve the proposed method of the study, a hybrid optimization algorithm is developed, which combines the enthusiasm-assisted teaching and learning-based optimization with an enhanced version of particle swarm optimization (EaTLBO-EPSO). Various dynamic pricing strategies, including Time-of-Use (ToU) pricing for both utility and customer sides, Real-Time Pricing (RTP), and their combinations, are designed for implementation in deregulated electricity market settings. After the implementation of the proposed models, the following conclusions may be drawn:

- In Scenario 3, RTP pricing is shown to be the optimum pricing mechanism, with overall load and peak load reductions of 5.09% and 6.36%, respectively, and a 7.62% gain in profits for the utility business. Nonetheless, when RTP is combined with ToU outage costs and ToU participation factors on the customer side, the total load reduction and peak load reduction are enhanced to 6.11% and 7.73%, respectively. In addition, utility earnings grew by 4.93% in Scenario 4 compared to Scenario 1.
- In Scenario 5, integrating RESs with the CC-GTDR and the Profit-based DCEED resulted in an 8.55% improvement in utility profit. On the other hand, compared to the approach used in Scenario 4, it is less effective in terms of total load reduction and peak load reduction.
- After the implementation of RESs, the produced volume of NOx emissions is reduced by 11.20% and 17.19% as compared to Scenario 1 and Base Case (Fixed EP), respectively. However, it has been achieved at the cost of a 6.83% and 6.76% increase in reserve cost (in comparison to Scenario 1 and Base Case (Fixed EP)) because of the higher requirement of SRR to handle the volatility of RESs.

7.2 Future Works

The successful implementation of the proposed CC-GTDR in this study demonstrates the potential for further advancements and applications in the field of demand response management. In light of the study's findings and conclusions, the following directions for future research can be identified:

1) <u>Integration of electric vehicles (EVs):</u> As the adoption of electric vehicles continues to grow, investigating the impact of EV charging and discharging on demand response programs and the

power grid is essential. Future research could extend the proposed CC-GTDR to incorporate EVs as a flexible resource for demand-side management, facilitating vehicle-to-grid (V2G) interactions.

2) Expansion to distributed energy resources (DERs): The CC-GTDR can be extended to accommodate various distributed energy resources, such as solar panels, wind turbines, and energy storage systems. By incorporating DERs, the demand response program can further enhance grid flexibility, reliability, and support higher levels of renewable energy integration.
3) Application to microgrids and virtual power plants (VPPs): The proposed CC-GTDR could be adapted for application in microgrids and virtual power plants, which can provide additional flexibility and resilience to the power system by managing the operation of distributed energy resources and controllable loads.
4) Development of adaptive and learning algorithms: Future research could focus on designing adaptive and learning algorithms for the CC-GTDR to better predict and respond to changing customer behavior, grid conditions, and market dynamics. This would enhance the effectiveness of the demand response program over time and facilitate more efficient grid operation.
5) Investigation of cyber-security and privacy concerns: As the proposed CC-GTDR relies on the collection and processing of customer data, addressing potential cyber-security and privacy challenges is essential. Future studies could explore methods for ensuring data security and privacy while maintaining the effectiveness of the demand response program.
6) Evaluation of the impact of different regulatory frameworks: As the power sector evolves, regulatory frameworks will need to adapt to facilitate the deployment of innovative demand response programs like the CC-GTDR. Future research could evaluate the impact of various regulatory frameworks on the effectiveness and adoption of the proposed demand response program.

By exploring these future research directions, the potential of the proposed CC-GTDR can be further harnessed to improve the flexibility, efficiency, and resilience of power systems, facilitating the integration of renewable energy sources, and fostering a sustainable energy future.

Appendix

In the following section, we present the comprehensive dataset utilized for executing the simulations pertinent to this research. This data encompasses a wide array of information and characteristics including, but not limited to, the operating limitations, cost factors, and emissions profiles of power generators. Moreover, it encapsulates considerations related to transmission line losses, diurnal load profiles, and customer-centric information. Additionally, the data set comprises pertinent details concerning renewable energy sources such as wind turbine generators and photovoltaic solar modules.

We believe that the accessibility of this data and information will enable readers to replicate the results of this study with precision. Furthermore, it is anticipated to serve as a catalyst for the advancement of the underlying formulation and concept presented in this research, thus facilitating the elevation of this study to the subsequent stage.

Table A.1 delineates the operating limits, cost parameters, and emissions characteristics of the 10-unit system generators. Table A.2 offers an overview of the ramp rates and Prohibited Operating Zone (POZ) data corresponding to the same 10-unit system. Table A.3 presents the B-coefficients responsible for transmission power losses within the 10-unit system.

Table A.1: Generators' operating limits, cost, and emissions characteristics – 10 units system

$\boldsymbol{Unit}$	$\boldsymbol{P_{min}}$	$\boldsymbol{P_{max}}$	$\boldsymbol{a}(\$/\boldsymbol{h})$	$\boldsymbol{b}(\$/\boldsymbol{MWh})$	$\boldsymbol{c}(\$/(\boldsymbol{MW})^{\boldsymbol{2h}})$	$\boldsymbol{d}(\$/\boldsymbol{h})$	$\boldsymbol{e}(\boldsymbol{rad}/\boldsymbol{MW})$	$\boldsymbol{\alpha_{NO_x}}(\boldsymbol{lb}/\boldsymbol{h})$	$\boldsymbol{\beta_{NO_x}}(\boldsymbol{lb}/\boldsymbol{MWh})$	$\boldsymbol{\gamma_{NO_x}}(\boldsymbol{lb}/(\boldsymbol{MW})^{\boldsymbol{2h}})$	$\boldsymbol{\eta_{NO_x}}(\boldsymbol{lb}/\boldsymbol{h})$	$\boldsymbol{\delta_{NO_x}}(\boldsymbol{1}/\boldsymbol{MW})$
1	10	55	1000.403	40.5407	0.12951	33	0.0174	360.0012	−3.9864	0.04702	0.25475	0.01234
2	20	80	950.606	39.5804	0.10908	25	0.0178	350.0056	−3.9524	0.04652	0.25475	0.01234
3	47	120	900.705	36.5104	0.12511	32	0.0162	330.0056	−3.9023	0.04652	0.25163	0.01215
4	20	130	800.705	39.5104	0.12111	30	0.0168	330.0056	−3.9023	0.04652	0.25163	0.01215
5	50	160	756.799	38.539	0.15247	30	0.0148	13.8593	0.3277	0.0042	0.2497	0.012
6	70	240	451.325	46.1592	0.10587	20	0.0163	13.8593	0.3277	0.0042	0.2497	0.012
7	60	300	1243.531	38.3055	0.03546	20	0.0152	40.2669	−0.5455	0.0068	0.248	0.0129
8	70	340	1049.998	40.3965	0.02803	30	0.0128	40.2669	−0.5455	0.0068	0.2499	0.01203
9	135	470	1658.569	36.3278	0.02111	60	0.0136	42.8955	−0.5112	0.0046	0.2547	0.01234
10	150	470	1356.659	38.2704	0.01799	40	0.0141	42.8955	−0.5112	0.0046	0.2547	0.01234

Table A.2: Generators' ramp rates and POZ information – 6 units system

$\boldsymbol{Unit}$	$\boldsymbol{DR}(\boldsymbol{MW}/\boldsymbol{h})$	$\boldsymbol{UR}(\boldsymbol{MW}/\boldsymbol{h})$	$\boldsymbol{P^0}(\boldsymbol{MW}/\boldsymbol{h})$	$\boldsymbol{POZ}(\boldsymbol{MW})$
1	50	50	20	[12 17] [35 45]
2	50	50	30	[0 0] [0 0]
3	50	50	105	[20 30] [40 45]
4	80	80	105	[0 0] [0 0]
5	80	80	95	[0 0] [0 0]
6	80	80	100	[0 0] [0 0]
7	80	80	100	[0 0] [0 0]
8	110	110	100	[0 0] [0 0]
9	150	110	400	[90 110] [240 250]
10	150	110	400	[150 165] [448 453]

Table A.11: Transmission power losses B-coefficients – 10 units systems

0.000049	0.000014	0.000015	0.000015	0.000016	0.000017	0.000017	0.000018	0.000019	0.00002
0.000014	0.000045	0.000016	0.000016	0.000017	0.000015	0.000015	0.000016	0.000018	0.000018
0.000015	0.000016	0.000039	0.00001	0.000012	0.000012	0.000014	0.000014	0.000016	0.000016
0.000015	0.000016	0.00001	0.00004	0.000014	0.00001	0.000011	0.000012	0.000014	0.000015
0.000016	0.000017	0.000012	0.000014	0.000035	0.000011	0.000013	0.000013	0.000015	0.000016
0.000017	0.000015	0.000012	0.00001	0.000011	0.000036	0.000012	0.000012	0.000014	0.000015
0.000017	0.000015	0.000014	0.000011	0.000013	0.000012	0.000038	0.000016	0.000016	0.000018
0.000018	0.000016	0.000014	0.000012	0.000013	0.000012	0.000016	0.00004	0.000015	0.000016
0.000019	0.000018	0.000016	0.000014	0.000015	0.000014	0.000016	0.000015	0.000042	0.000019
0.00002	0.000018	0.000016	0.000015	0.000016	0.000015	0.000018	0.000016	0.000019	0.000044

Table A.4 exhibits the power output of Intermittent Renewable Energy Sources (IRESs) alongside their respective forecasted power values. Table A.5 documents the hourly load demand data for 10-unit systems.

Table A.4: IRESs power output with their respective forecasted power

Time (h)	***Wind Farms Power Output (MW)***		***Solar Arrays Power Output (MW)***	
	Actual Power	***Forecasted Power***	***Actual Power***	***Forecasted Power***
1	27.72	13.49	0.00	0.00
2	70.34	53.79	0.00	0.00
3	12.90	16.68	0.00	0.00
4	128.59	150.85	0.00	0.00
5	225.47	239.88	0.00	0.00
6	378.30	395.48	6.64	11.50
7	338.68	262.66	26.95	39.71
8	66.63	52.40	67.45	74.41
9	120.22	96.51	116.32	124.29
10	208.20	164.33	131.12	135.56
11	302.63	320.85	153.26	156.13
12	32.51	12.90	161.60	181.30
13	223.96	232.28	162.05	178.01
14	121.40	125.57	154.41	168.86
15	30.78	33.79	142.94	134.59
16	272.46	285.13	106.36	99.80
17	156.18	198.57	91.40	91.55
18	402.35	383.29	32.88	24.08
19	276.20	203.74	1.67	1.54
20	346.78	381.52	0.00	0.00
21	252.80	204.48	0.00	0.00
22	177.60	228.49	0.00	0.00
23	139.81	62.66	0.00	0.00
24	228.49	166.40	0.00	0.00

Table A.5: Hourly load demand for 6- and 10-units' systems

10 Units - Time (h)	1	2	3	4	5	6	7	8	9	10	11	12
Load Demand (MW)	945	930	920	1100	1200	1300	1400	1480	1650	1700	1780	1800
10 Units - Time (h)	13	14	15	16	17	18	19	20	21	22	23	24
Load Demand (MW)	1845	1730	1550	1460	1420	1500	1580	1620	1650	1350	1160	1070

Table A.6 details the cost coefficients related to customers, customer types, participation factors, and daily power curtailments for each customer within Case 2. Additionally, the hourly power interruptibility values for Case 2 are illustrated in Figure A.1.

Table A.6: Customers cost coefficients, customers' types, customers' participation factors, and daily power curtailments for each customer – Case Study 2

$\boldsymbol{Customer\ (j)}$	$\boldsymbol{K_{1,j}}$	$\boldsymbol{K_{2,j}}$	$\boldsymbol{\theta_j}$	$\boldsymbol{CM_j(MW)}$
1	1.847	11.64	0.095	180
2	1.378	11.63	0.14	230
3	1.079	11.32	0.26	310
4	0.9124	11.50	0.37	390
5	0.8794	11.21	0.55	440
6	1.378	11.63	0.84	530
7	1.5231	11.50	1.00	600

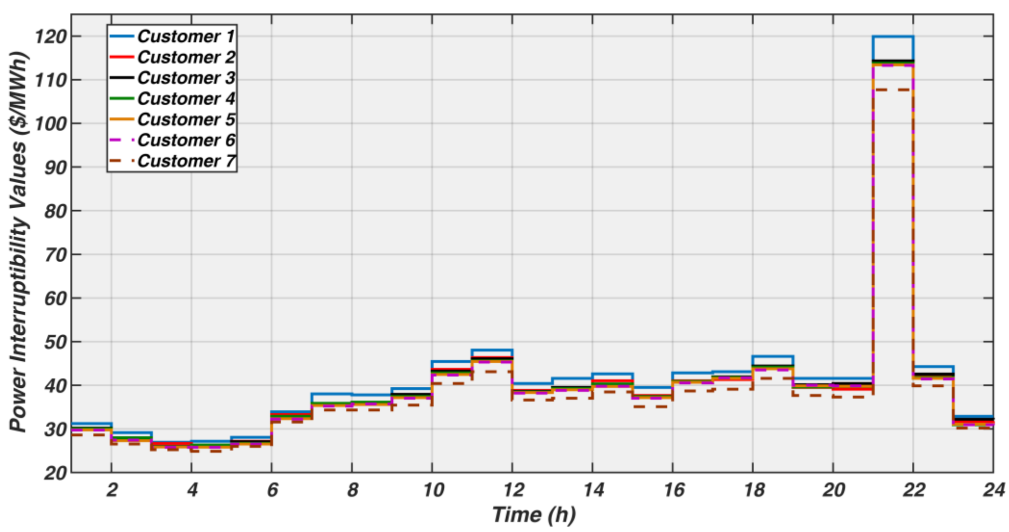

Figure A.1: The power interruptibility hourly values for the case study 2

Finally, the characteristics of wind turbine generators and photovoltaic (PV) modules are articulated in Tables A.7 and A.8, respectively. The power curve of the wind turbine generator is also visually represented in Figure A.2.

Table A.7: Utilized wind turbine generators' characteristics

Manufacturer	**Enercon**
Cut-in wind speed	2m/s
Rated wind speed	11.5m/s
Cut-out wind speed	25m/s
Diameter	115.7m
Swept area	10,515.5m²
Number of blades	3
Rotor max speed	12.8U/min
Power density 1	285.3W/m²
Power density 2	3.5m²/kW

Table A.8: Utilized photovoltaic (PV) modules' characteristics

Manufacturer	**SolarGate**
Power Rating (Pmpp)	220W
Maximum Current (Impp)	7.23A
Maximum Voltage (Vmpp)	30.29V
Short-circuit Current (Isc)	7.77A
Open-circuit Voltage (Voc)	36.42V
Efficiency Rating	14.29%
Power Tolerance	±3%
Temperature Range	40˚C to 85˚C
Damp Heat	85%RH
Static Load Front and Back	2400pascals
Front Loading	5400pascals
Hail Impact	25mm stainless ball at 23m.s
Dimensions	(L)1669mm x (W)986mm x (D)40mm

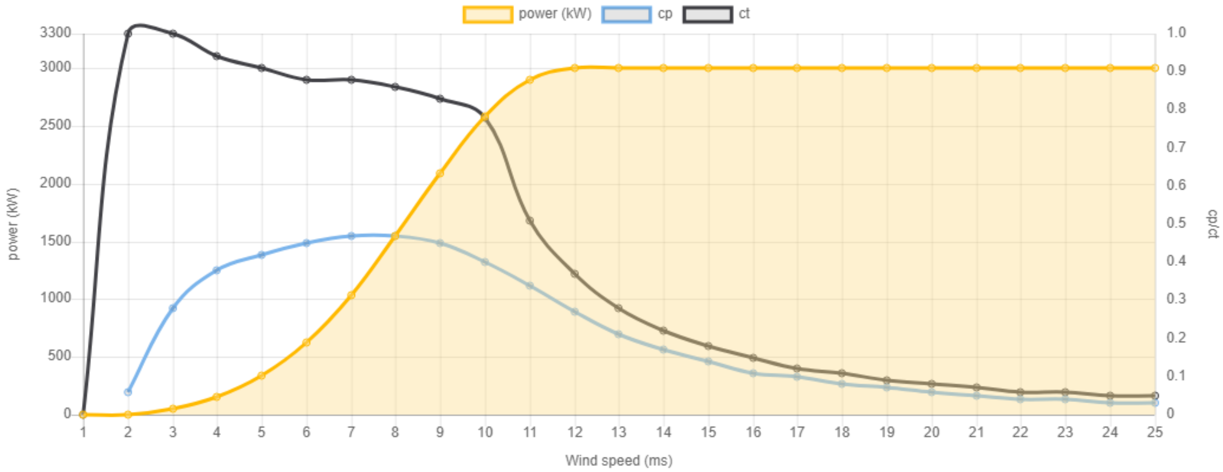

Figure A.2: The power curve of the used Enercon wind turbine generator

Bibliography

[1] D. Stanelyte, N. Radziukyniene, and V. Radziukynas, "Overview of demand-response services: A review," *Energies*, vol. 15, no. 5, p. 1659, 2022.

[2] H. T. Haider, O. H. See, and W. Elmenreich, "A review of residential demand response of smart grid," *Renewable and Sustainable Energy Reviews*, vol. 59, pp. 166-178, 2016.

[3] V. M. Balijepalli, V. Pradhan, S. A. Khaparde, and R. Shereef, "Review of demand response under smart grid paradigm," in *ISGT2011-India*, 2011, pp. 236-243: IEEE.

[4] M. H. Shoreh, P. Siano, M. Shafie-khah, V. Loia, and J. P. Catalão, "A survey of industrial applications of Demand Response," *Electric Power Systems Research*, vol. 141, pp. 31-49, 2016.

[5] J. S. Vardakas, N. Zorba, and C. V. Verikoukis, "A survey on demand response programs in smart grids: Pricing methods and optimization algorithms," *IEEE Communications Surveys & Tutorials*, vol. 17, no. 1, pp. 152-178, 2014.

[6] G. Le Ray, E. M. Larsen, and P. Pinson, "Evaluating price-based demand response in practice—with application to the EcoGrid EU Experiment," *IEEE Transactions on Smart Grid*, vol. 9, no. 3, pp. 2304-2313, 2016.

[7] Q. Shi, C.-F. Chen, A. Mammoli, and F. Li, "Estimating the profile of incentive-based demand response (IBDR) by integrating technical models and social-behavioral factors," *IEEE Transactions on Smart Grid*, vol. 11, no. 1, pp. 171-183, 2019.

[8] T. H. Christensen *et al.*, "The role of competences, engagement, and devices in configuring the impact of prices in energy demand response: Findings from three smart energy pilots with households," *Energy Policy*, vol. 137, p. 111142, 2020.

[9] M. H. Amini *et al.*, "Demand response in future power networks: panorama and state-of-the-art," *Sustainable Interdependent Networks II: From Smart Power Grids to Intelligent Transportation Networks*, pp. 167-191, 2019.

[10] B. Shen, G. Ghatikar, Z. Lei, J. Li, G. Wikler, and P. Martin, "The role of regulatory reforms, market changes, and technology development to make demand response a viable resource in meeting energy challenges," *Applied Energy*, vol. 130, pp. 814-823, 2014.

[11] D. Hurley, P. Peterson, and M. Whited, "Demand response as a power system resource," *Synapse Energy Economics Inc*, 2013.

[12] A. Davoodi, A. R. Abbasi, and S. Nejatian, "Multi-objective techno-economic generation expansion planning to increase the penetration of distributed generation resources based on demand response algorithms," *International Journal of Electrical Power & Energy Systems*, vol. 138, p. 107923, 2022.

[13] K. Gamma, R. Mai, C. Cometta, and M. Loock, "Engaging customers in demand response programs: The role of reward and punishment in customer adoption in Switzerland," *Energy Research & Social Science*, vol. 74, p. 101927, 2021.

[14] A. Jafari, T. Khalili, H. G. Ganjehlou, and A. Bidram, "Optimal integration of renewable energy sources, diesel generators, and demand response program from pollution, financial, and reliability viewpoints: A multi-objective approach," *Journal of cleaner production*, vol. 247, p. 119100, 2020.

[15] E. Sarker *et al.*, "Progress on the demand side management in smart grid and optimization approaches," *International Journal of Energy Research*, vol. 45, no. 1, pp. 36-64, 2021.

[16] E. Maglakelidze and M. Veshaguri, "Some Considerations in Respect to Customer-Centric Demand Response Market Design," in *Proceedings of International Academic Conferences*, 2017, no. 5808117: International Institute of Social and Economic Sciences.

[17] G. Lahoti, D. Mashima, and W.-P. Chen, "Customer-centric energy usage data management and sharing in smart grid systems," in *Proceedings of the first ACM workshop on Smart energy grid security*, 2013, pp. 53-64.

[18] R. Tang, S. Wang, and H. Li, "Game theory based interactive demand side management responding to dynamic pricing in price-based demand response of smart grids," *Applied Energy*, vol. 250, pp. 118-130, 2019.

[19] C. Feng, Z. Li, M. Shahidehpour, F. Wen, and Q. Li, "Stackelberg game based transactive pricing for optimal demand response in power distribution systems," *International Journal of Electrical Power & Energy Systems*, vol. 118, p. 105764, 2020.

[20] M. Yu and S. H. Hong, "Incentive-based demand response considering hierarchical electricity market: A Stackelberg game approach," *Applied Energy*, vol. 203, pp. 267-279, 2017.

[21] Y. Li, C. Wang, G. Li, and C. Chen, "Optimal scheduling of integrated demand response-enabled integrated energy systems with uncertain renewable generations: A Stackelberg game approach," *Energy Conversion and Management*, vol. 235, p. 113996, 2021.

[22] G. Wang *et al.*, "Study on the promotion impact of demand response on distributed PV penetration by using non-cooperative game theoretical analysis," *Applied energy*, vol. 185, pp. 1869-1878, 2017.

[23] M. Gaba and S. Chanana, "A non-cooperative game based energy management considering distributed energy resources in price-based and incentive-based demand response program," *International Journal of Emerging Electric Power Systems*, vol. 22, no. 6, pp. 807-830, 2021.

[24] N. Guo, Y. Wang, and G. Yan, "A double-sided non-cooperative game in electricity market with demand response and parameterization of supply functions," *International Journal of Electrical Power & Energy Systems*, vol. 126, p. 106565, 2021.

[25] H. R. Bokkisam, R. M. Acharya, and M. Selvan, "Framework of transactive energy market pool for community energy trading and demand response management using an auction-theoretic approach," *International Journal of Electrical Power & Energy Systems*, vol. 137, p. 107719, 2022.

[26] Z. Zhou, F. Liu, Z. Li, and H. Jin, "When smart grid meets geo-distributed cloud: An auction approach to datacenter demand response," in *2015 IEEE Conference on Computer Communications (INFOCOM)*, 2015, pp. 2650-2658: IEEE.

[27] D. Muthirayan, D. Kalathil, K. Poolla, and P. Varaiya, "Mechanism design for demand response programs," *IEEE Transactions on Smart Grid*, vol. 11, no. 1, pp. 61-73, 2019.

[28] Z. Zhang, Y. Huang, Z. Chen, and W.-J. Lee, "Integrated demand response for microgrids with incentive compatible bidding mechanism," *IEEE Transactions on Industry Applications*, 2022.

[29] J. Chen, D. Ye, Z. Liu, S. Ji, Q. He, and Y. Xiang, "A Truthful and near-optimal mechanism for colocation emergency demand response," *IEEE Transactions on Mobile Computing*, vol. 20, no. 9, pp. 2728-2744, 2020.

[30] S. Fan, Q. Ai, and L. Piao, "Bargaining-based cooperative energy trading for distribution company and demand response," *Applied energy*, vol. 226, pp. 469-482, 2018.

[31] N. Rahbari-Asr, U. Ojha, Z. Zhang, and M.-Y. Chow, "Incremental welfare consensus algorithm for cooperative distributed generation/demand response in smart grid," *IEEE Transactions on Smart Grid*, vol. 5, no. 6, pp. 2836-2845, 2014.

[32] B. Zhu, X. Xia, and Z. Wu, "Evolutionary game theoretic demand-side management and control for a class of networked smart grid," *Automatica*, vol. 70, pp. 94-100, 2016.

[33] P. A. Apostolopoulos, E. E. Tsiropoulou, and S. Papavassiliou, "Demand response management in smart grid networks: A two-stage game-theoretic learning-based approach," *Mobile Networks and Applications*, vol. 26, pp. 548-561, 2021.

[34] S. Abapour, B. Mohammadi-Ivatloo, and M. T. Hagh, "A Bayesian game theoretic based bidding strategy for demand response aggregators in electricity markets," *Sustainable Cities and Society*, vol. 54, p. 101787, 2020.

[35] X. Liu, B. Gao, C. Wu, and Y. Tang, "Demand-side management with household plug-in electric vehicles: A Bayesian game-theoretic approach," *IEEE Systems Journal*, vol. 12, no. 3, pp. 2894-2904, 2017.

[36] S. Nan, M. Zhou, and G. Li, "Optimal residential community demand response scheduling in smart grid," *Applied Energy*, vol. 210, pp. 1280-1289, 2018.

[37] R. Poudineh and T. Jamasb, "Distributed generation, storage, demand response and energy efficiency as alternatives to grid capacity enhancement," *Energy Policy,* vol. 67, pp. 222-231, 2014.

[38] M. Wang, H. Xu, S. Yang, L. Yang, R. Duan, and X. Zhou, "Non-cooperative differential game based energy consumption control for dynamic demand response in smart grid," *China Communications,* vol. 16, no. 8, pp. 107-114, 2019.

[39] Y. Zheng, J. Luo, X. Yang, and Y. Yang, "Intelligent regulation on demand response for electric vehicle charging: a dynamic game method," *IEEE Access,* vol. 8, pp. 66105-66115, 2020.

[40] J. Yang, T. Ma, K. Ma, Z. Tian, and Q. Zheng, "A cooperative demand response strategy based on repeated game and cartel mechanism," *Electric Power Systems Research,* vol. 201, p. 107475, 2021.

[41] M. Motalleb, A. Annaswamy, and R. Ghorbani, "A real-time demand response market through a repeated incomplete-information game," *Energy,* vol. 143, pp. 424-438, 2018.

[42] R. Elie, E. Hubert, T. Mastrolia, and D. Possamaï, "Mean–field moral hazard for optimal energy demand response management," *Mathematical Finance,* vol. 31, no. 1, pp. 399-473, 2021.

[43] A. Marín Radoszynski and P. Pinson, "Electric demand response and bounded rationality: mean-field control for large populations of heterogeneous bounded-rational agents," *Philosophical Transactions of the Royal Society A,* vol. 379, no. 2202, p. 20190429, 2021.

[44] J. R. Vázquez-Canteli and Z. Nagy, "Reinforcement learning for demand response: A review of algorithms and modeling techniques," *Applied energy,* vol. 235, pp. 1072-1089, 2019.

[45] B. Wang, Y. Li, W. Ming, and S. Wang, "Deep reinforcement learning method for demand response management of interruptible load," *IEEE Transactions on Smart Grid,* vol. 11, no. 4, pp. 3146-3155, 2020.

[46] X. Zhang, R. Lu, J. Jiang, S. H. Hong, and W. S. Song, "Testbed implementation of reinforcement learning-based demand response energy management system," *Applied energy,* vol. 297, p. 117131, 2021.

[47] X. Yan, Y. Ozturk, Z. Hu, and Y. Song, "A review on price-driven residential demand response," *Renewable and Sustainable Energy Reviews,* vol. 96, pp. 411-419, 2018.

[48] C. Ibrahim, I. Mougharbel, H. Y. Kanaan, N. Abou Daher, S. Georges, and M. Saad, "A review on the deployment of demand response programs with multiple aspects coexistence over smart grid platform," *Renewable and Sustainable Energy Reviews*, vol. 162, p. 112446, 2022.

[49] N. Lashmar, B. Wade, L. Molyneaux, and P. Ashworth, "Motivations, barriers, and enablers for demand response programs: A commercial and industrial consumer perspective," *Energy Research & Social Science*, vol. 90, p. 102667, 2022.

[50] D. Koolen, N. Sadat-Razavi, and W. Ketter, "Machine learning for identifying demand patterns of home energy management systems with dynamic electricity pricing," *Applied Sciences,* vol. 7, no. 11, p. 1160, 2017.

[51] R. Sharifi, A. Anvari-Moghaddam, S. Hamid Fathi, J. M. Guerrero, and V. Vahidinasab, "An optimal market-oriented demand response model for price-responsive residential consumers," *Energy Efficiency,* vol. 12, pp. 803-815, 2019.

[52] A. Dadkhah, B. Vahidi, M. Shafie-khah, and J. P. Catalão, "Power system flexibility improvement with a focus on demand response and wind power variability," *IET Renewable Power Generation,* vol. 14, no. 6, pp. 1095-1103, 2020.

[53] M. Azimian, V. Amir, R. Habibifar, and H. Golmohamadi, "Probabilistic optimization of networked multi-carrier microgrids to enhance resilience leveraging demand response programs," *Sustainability,* vol. 13, no. 11, p. 5792, 2021.

[54] S. Heinen and P. Richards, "Towards customer-centric energy utilities-A granular data-driven bottom-up approach to understanding energy customer trends," *The Electricity Journal,* vol. 33, no. 9, p. 106836, 2020.

[55] M. Jäntti, A. Jäntti, and M. Shafie-khah, "Toward customer-centric power grid: Residential EV charging simulator for smart homes," in *Decentralized Frameworks for Future Power Systems*: Elsevier, 2022, pp. 207-226.

[56] J. Price, S. Gulati, J. Lehr, and S. Penn, "The Benefits and Costs of US Air Pollution Regulations," *Cambridge, MA, May*, 2020.

[57] A. Goudarzi, Y. Li, and J. Xiang, "Efficient energy management of renewable resources in microgrids," in *Renewable energy microgeneration systems*: Elsevier, 2021, pp. 285-321.

[58] A. Goudarzi, C. Zhang, S. Fahad, and A. J. Mahdi, "A hybrid sequential approach for solving environmentally constrained optimal scheduling in co-generation systems," *Energy Reports*, vol. 7, pp. 3460-3479, 2021.

[59] C. Lin and C. H. Twu, "Fuzzy MCDM for evaluating fashion trend alternatives," *International Journal of Clothing Science and Technology*, 2012.

[60] X. Ji, H. Ye, J. Zhou, Y. Yin, and X. Shen, "An improved teaching-learning-based optimization algorithm and its application to a combinatorial optimization problem in foundry industry," *Applied Soft Computing*, vol. 57, pp. 504-516, 2017.

[61] X. Chen, B. Xu, K. Yu, and W. Du, "Teaching-learning-based optimization with learning enthusiasm mechanism and its application in chemical engineering," *Journal of Applied Mathematics*, vol. 2018, 2018.

[62] F. Marini and B. Walczak, "Particle swarm optimization (PSO). A tutorial," *Chemometrics and Intelligent Laboratory Systems*, vol. 149, pp. 153-165, 2015.

[63] Y. Zhang, S. Wang, and G. Ji, "A comprehensive survey on particle swarm optimization algorithm and its applications," *Mathematical problems in engineering*, vol. 2015, 2015.

[64] C. Le Thanh, T. Sang-To, H.-L. Hoang-Le, T.-T. Danh, S. Khatir, and M. A. Wahab, "Combination of intermittent search strategy and an improve particle swarm optimization algorithm (IPSO) for damage detection of steel frame," *Frattura ed Integrità Strutturale*, vol. 16, no. 59, pp. 141-152, 2022.

[65] A. Goudarzi, Y. Li, S. Fahad, and J. Xiang, "A Game Theory-Based Interactive Demand Response for Handling Dynamic Prices in Security-Constrained Electricity Markets," *Sustainable Cities and Society*, p. 103073, 2021.

[66] N. I. Nwulu and X. Xia, "Implementing a model predictive control strategy on the dynamic economic emission dispatch problem with game theory based demand response programs," *Energy*, vol. 91, pp. 404-419, 2015.